AFRPL TR-83-013 AD:

AD A131007

Particle Impact Erosion

Volume III: User's Manual Chamber Flowfield Code (CFC) and Charring Material Ablation-Erosion (CMAE) Code

User's Manual
for the period
1 February 1979 to
31 December 1981

May 1983

Authors:
Z. Chiba
R. Beck

Acurex Corporation
Aerotherm Division
485 Clyde Avenue
Mountain View, CA 94042

F04611-79-C-0012

Approved for Public Release

Distribution unlimited. The AFRPL Technical Services Office has reviewed this report, and it is releasable to the National Technical Information Service, where it will be available to the general public, including foreign nationals.

DTIC ELECTE AUG 0 2 1983 S E D

DTIC FILE COPY

prepared for the: **Air Force Rocket Propulsion Laboratory**

Air Force Space Technology Center
Space Division, Air Force Systems Command
Edwards Air Force Base,
California 93523

3-5-16-1 C

83 08 01 060

NOTICES

When U.S. Government drawings, specifications, or other data are used for any purpose other than a definitely related government procurement operation, the Government thereby incurs no responsibility nor obligation whatsoever, and the fact that the Government may have formulated, furnished, or in any way supplied the said drawings, specifications or other data, is not to be regarded by implication or otherwise, or in any manner licensing the holder or any person or corporation, or conveying any rights or permission to manufacture, use or sell any patented invention that may in any way be related thereto.

FOREWORD

This report was submitted by Acurex Corporation/Aerotherm Division, 485 Clyde Avenue, Mountain View, California 94042, under Contract F04611-79-C-0012, Job Order No. 305909JZ with the Air Force Rocket Propulsion Laboratory, Edwards AFB, California 93523.

This technical report is approved for release and distribution in accordance with the distribution statement on the cover and on DD Form 1473.

RAFAEL FELIX
Chief, Space Propulsion Section

FOR THE DIRECTOR

THOMAS MEIER, Colonel, USAF
Director, Solid Rocket Division

LEE MEYER
Chief, Ballistic Missile and
Space Propulsion Branch

DTIC COPY INSPECTED 2

Accession For
NTIS GRA&I [X]
DTIC TAB [ ]
Unannounced [ ]
Justification
By
Distribution/
Availability Codes
Dist Avail and/or Special
A

UNCLASSIFIED

SECURITY CLASSIFICATION OF THIS PAGE (When Data Entered)

REPORT DOCUMENTATION PAGE		READ INSTRUCTIONS BEFORE COMPLETING FORM
1. REPORT NUMBER AFRPL-TR-83-0013	2. GOVT ACCESSION NO.	3. RECIPIENT'S CATALOG NUMBER
4. TITLE (and Subtitle) Particle Impact Erosion Volume III: User's Manual -- Chamber Flowfield Code (CFC) and Charring Material Ablation-Erosion (CMAE) Code		5. TYPE OF REPORT & PERIOD COVERED User's Manual 1 Feb. 1979 to 31 Dec. 1981 6. PERFORMING ORG. REPORT NUMBER UM-82-15/ATD
7. AUTHOR(s) Z. Chiba, R. Beck		8. CONTRACT OR GRANT NUMBER(s) F04611-79-C-0012
9. PERFORMING ORGANIZATION NAME AND ADDRESS Acurex Corporation/Aerotherm Division 485 Clyde Avenue Mountain View, California 94042		10. PROGRAM ELEMENT, PROJECT, TASK AREA & WORK UNIT NUMBERS
11. CONTROLLING OFFICE NAME AND ADDRESS Air Force Rocket Propulsion Laboratory, MKBS Edwards Air Force Base, California 93523		12. REPORT DATE May 1983 13. NUMBER OF PAGES 110
14. MONITORING AGENCY NAME & ADDRESS(if different from Controlling Office)		15. SECURITY CLASS. (of this report) Unclassified 15a. DECLASSIFICATION/DOWNGRADING SCHEDULE

16. DISTRIBUTION STATEMENT (of this Report)
Approved for public release; distribution unlimited

17. DISTRIBUTION STATEMENT (of the abstract entered in Block 20, if different from Report)

18. SUPPLEMENTARY NOTES

19. KEY WORDS (Continue on reverse side if necessary and identify by block number)

rocket nozzle	numerical solution
ablation-erosion	particle streamlines
recession	particle impact
chamber flowfield	

20. ABSTRACT (Continue on reverse side if necessary and identify by block number)

An experimental and analytical program was conducted to develop a methodology to predict total recession, including the contribution by particulate impact erosion, in solid propellant rocket nozzles. The program was divided into two phases. Under Phase I, a methodology was developed for predicting recession due to particle impact erosion in the expansion (exit cone) region of nozzles. This phase was performed by the Aerojet Strategic

DD FORM 1 JAN 73 1473 EDITION OF 1 NOV 65 IS OBSOLETE

UNCLASSIFIED

SECURITY CLASSIFICATION OF THIS PAGE (When Data Entered)

Propulsion Company (ASPC) under a subcontract to the Aerotherm Division of Acurex Corporation. Under Phase II, a methodology was developed for predicting recession due to erosion coupled with ablation in the entrance and throat regions of nozzles. This phase was performed by Aerotherm.

For the supersonic expansion region methodology (Phase I), the TD2P computer code, contained within the Interim Solid Performance Program (ISPP), was chosen for predicting the two-phase flow. The TD2P code is used to predict the location of particle impingement on the nozzle exit cone wall and the impact conditions. Also, it was used in conjunction with erosion test data to generate mechanical erosion models. Data for erosion models were obtained from one series of tests in the Dust Erosion Tunnel (DET) at the Arnold Engineering Development Center (AEDC) and a second series of tests in small rocket motors at ASPC. Two independent mechanical erosion models were developed. The first was derived using the "G-law" approach, while the second was formulated to represent the physical phenomena occurring during the erosion process.

For the subsonic entrance and throat region methodology (Phase II), a variety of tests were used in modeling particle impact erosion -- particle (droplet) breakup; aluminum (Al) and aluminum oxide (Al_2O_3) chemical reactions with carbon; and subsonic erosion tests using Al and Al_2O_3 impacting a carbon surface. The subsonic erosion was modeled using the "G-law" approach. Two computer codes were developed: (1) the Chamber Flowfield Code (CFC) for predicting particle impact conditions at the nozzle wall, and (2) the Charring Material Ablation-Erosion (CMAE) code for computing the contributions of erosion and ablation to recession.

Both the Phase I and Phase II recession prediction methodologies were demonstrated by comparing predictions to data from rocket motor test firings having known or suspected particle impact erosion. Program results are reported in four volumes, as follows:

- Volume I: Recession Prediction Methodology for Rocket Nozzle Entrance and Throat Regions
- Volume II: Erosion Model Development (Expansion Region)
- Volume III: User's Manual -- Chamber Flowfield Code (CFC) and Charring Material Ablation-Erosion (CMAE) Code
- Volume IV: User's Manual -- Erosion Prediction Procedure for Rocket Nozzle Expansion Region

TABLE OF CONTENTS

Section		Page
	SUMMARY	5
1	INTRODUCTION	9
	1.1 Part 1 -- Chamber Flowfield Code	9
	1.2 Part 2 -- Charring Material Ablation-Erosion (CMAE) Code	11
2	CFC ANALYTICAL BASIS	15
	2.1 Geometry	16
	2.2 Boundary Conditions in the Chamber	19
	2.3 Particle Trajectory Calculations	27
3	CFC OVERALL STRUCTURE	37
4	SPP INPUT CHANGES FOR CFC	41
	4.1 SPP Namelist	41
	4.2 TD2 Namelist	42
5	NEW INPUT VARIABLES FOR CFC	49
6	NEW OUTPUT FOR CFC	61
7	SAMPLE PROBLEM USING CFC	73
8	CMAE ANALYTICAL BASIS	89
9	CMAE INPUT	95
10	SAMPLE PROBLEM USING CMAE	99
11	REFERENCES	109

LIST OF ILLUSTRATIONS

Figure		Page
1	Mesh Generation Options	17
2	Comparison of Overall Structures of SPP and CFC	38
3	Axisymmetric Approximation of Non-Axisymmetric Grain Configurations	50
4	Chamber and Grain Configuration Schematic	52
5	CFC Mesh Geometry for the NTF 001 at 0 Sec Burn Time	84
6	Particle Trajectories for the NTF 001 Demonstration at 0 Sec Burn Time	85

LIST OF TABLES

Table		Page
1	Input Data Set Description	39
2	Example of Particle Impact Conditions Table Printout	62
3	Description of Variables in Particle Impact Conditions Table	63
4	Example of L(old) - L(new) Matrix Printout	65
5	Example of ROP-YP and Other Arrays Printout	66
6	Example of Particle Integration Calculations Table . .	68
7	Example of WPSCDL and DMDOT Arrays at the Inflow Boundary	70
8	Example of Table of Boundary Conditions at Mesh Point	70
9	Examples of Particle Trajectory Calculations Error Messages	71
10	CFC Sample Problem Input	74
11	ACE Run Results Used in Sample Problem	75
12	CFC Sample Problem Output	76
13	CMAE Sample Problem Input	100
14	CMAE Sample Problem Output	103

SUMMARY

An experimental and analytical program was conducted to develop a methodology to predict total recession, including the contribution by particulate impact erosion, in solid propellant rocket nozzles. The program was divided into two phases. Under Phase I, a methodology was developed for predicting recession due to particle impact erosion in the expansion (exit cone) region of nozzles. This effort was performed by the Aerojet Strategic Propulsion Company (ASPC) under a subcontract to the Aerotherm Division of Acurex Corporation. Under Phase II, a methodology was developed for predicting recession due to erosion coupled with ablation in the entrance and throat regions of nozzles. This effort was performed by Aerotherm.

Results from this program are reported in four separate volumes, as follows:

- Volume I: Recession Prediction Methodology for Rocket Nozzle Entrance and Throat Regions (Reference 1)
- Volume II: Erosion Model Development (Expansion Region) (Reference 2)
- Volume III: User's Manual -- Chamber Flowfield Code (CFC) and Charring Material Ablation-Erosion (CMAE) Code
- Volume IV: User's Manual -- Erosion Prediction Procedure for Rocket Nozzle Expansion Region (Reference 3)

PREVIOUS PAGE IS BLANK

The remainder of this summary provides a brief overview of the recession prediction methodologies developed for the nozzle expansion region (reported in Volume II) and for the nozzle entrance and throat regions (reported in Volume I).

Nozzle Expansion Region

A procedure was developed for predicting the erosion that occurs in a solid rocket nozzle exit cone when aluminum oxide (Al_2O_3) particles in the flow impact the nozzle wall in the supersonic region downstream of the nozzle throat. This procedure consists of a two-phase flow solution and two independent mechanical erosion models. These models calculate the nozzle wall erosion patterns in carbon-carbon and bulk graphite materials as a function of the impinging particle flow properties, the impact angle, and the nozzle wall material properties.

An empirical "G-law" erosion model was developed for nozzle expansion regions from Dust Erosion Tunnel (DET) test data and small solid motor firing data. Specimens of carbon-carbon, bulk graphite, and tantalum/tungsten were exposed to particle-laden test gases. A debris layer shielding erosion model was also developed for the expansion region. In contrast to the empirical G-law, this model was formulated to represent the fundamental physics of the erosion process.

The TD2P two-phase flow code contained in the Interim Solid Performance Program (ISPP) was modified to incorporate the above two erosion models. This version of TD2P constitutes the methodology for predicting particle impact conditions at the walls of nozzle exit cones and the resulting wall erosion. Predictions were made using both erosion models for various solid rocket motor test firings where erosion occurred. Predictions using the G-law model were generally acceptable relative to test results, providing the particle flow and

impact conditions were within the range covered by the DET and small motor experiments. Predictions using the debris layer model were also generally satisfactory, but not as accurate as G-law predictions when particle impact conditions were within the DET and small motor test range. However, the debris layer model was the most accurate for conditions outside the experimental range.

Nozzle Entrance and Throat Regions

A methodology was developed for predicting the total recession, including particle impact erosion, for the entrance and throat regions of solid rocket nozzles. Major program efforts included the development of a motor chamber-nozzle flowfield code and a model for describing the erosion process in the subsonic regions of the nozzle.

The Fully Coupled Transonic (FCT) two-phase flow module of the Solid Performance Prediction (SPP) program (Reference 4) was modified to compute particle trajectory crossovers and particle impact conditions at the nozzle wall. Also, the calculation domain was extended forward to account for the motor chamber and propellant grain, including mass injection from the grain. However, flow within the submerged region of nozzles remains to be included. This modification is referred to as the Chamber Flowfield Code (CFC).

Empirical subsonic erosion models were developed for predicting recession due to the impact of aluminum (Al) and Al_2O_3 particles. Models were constructed in the form of a G-law with two components: mechanical erosion due to mechanical mass removal and chemical erosion due to particle-surface chemical reactions. However, the models are based on bulk graphite data and provide only rough estimates for the erosion of carbon-carbon composites. The Charring Material Ablation (CMA) code (Reference 5) was modified to include these models in predictions of recession resulting from ablation and erosion.

This modification is designated the Charring Material Ablation-Erosion (CMAE) code.

The recession prediction methodology for subsonic flow regimes was demonstrated for two motor firings having suspected particle erosion in the entrance region of carbon-carbon composite nozzles. The demonstration results substantiated the prediction of the onset of particle impact for the two motors. However, recession predictions using the bulk graphite erosion model provided only a rough estimate of material removed.

Although not currently included in the recession prediction methodology, particle breakup in nozzle entrance and throat regions was modeled in terms of Bond number and nondimensional time. This model was based upon cold-flow data, and its applicability to hot-firing conditions has not been demonstrated.

SECTION 1

INTRODUCTION

Described herein are the input and output features of two analytical procedures developed under the Particle Impact Erosion Program: The Chamber Flowfield Code (CFC) and the Charring Material Ablation-Erosion (CMAE) code. These two codes are key constituents of the methodology for predicting total recession, including the effects of particulate erosion, in the subsonic and transonic regions of solid propellant rocket nozzles. Details of the methodology are given in Volume I of the Particle Impact Erosion Program Final Report (Reference 1). This report is divided into two parts, as follows.

1.1 PART 1 -- CHAMBER FLOWFIELD CODE

Part 1 is a user's manual for the Chamber Flowfield Code (CFC), which calculates particle impact conditions in the entrance and throat regions of solid propellant rocket nozzles. CFC is an extension of the Fully Coupled Transonic (FCT) module of the Solid Performance Program (SPP). It is presumed that the user is thoroughly familiar with the use of the FCT module of the SPP code. Since the basic features of the FCT module are preserved in CFC, this manual should be used in conjunction with the SPP user's manual (Reference 4). Only modifications to the SPP input-output procedure are detailed herein. Major modifications made to the FCT code as part of the CFC development are described below.

Geometry

The calculation domain was extended forward into the chamber to account for the effects of chamber and grain configuration on particle impact conditions. As in FCT, only axisymmetric geometries are allowed, and the flow within the submerged region near the backside of the nozzle is not computed. However, the effects of the flow from the submerged region are treated in an approximate manner. Also, complex prepellant geometries, such as those with star grains and slots, can only be treated approximately with the code.

Boundary Conditions

The boundary conditions were modified to handle a specified mass flux and/or a grain burn-rate distribution along the input chamber-grain boundary. If the chamber has a front-end closure (with no mass injection), the code can treat that boundary separately using slip-flow conditions.

Particle Flow Calculations

The particle trajectory calculations were modified to allow for impact at the wall, particle trajectory crossover, and particles crossing the nozzle axis. Locations of particle impact on the wall are identified for each particle size group, and the distributions of particle impingement velocity, angle, density and mass flux along the wall are output. The particle size distribution calculations were also modified. For erosion calculations the large aluminum particles coming off the grain are of more interest than the smaller aluminum oxide particles formed in the chamber. Hence, CFC includes an option to calculate the mean diameter and size distribution of the aluminum agglomerates leaving the grain surface. Presently, as in FCT, the CFC code does not account for particle size change mechanisms.

1.2 PART 2 -- CHARRING MATERIAL ABLATION-EROSION (CMAE) CODE

Part 2 is a user's manual for the Charring Material Ablation-Erosion (CMAE) code. This code calculates the total recession, including erosion due to particle impact, and one-dimensional in-depth transient conduction in rocket nozzle materials. CMAE is an extension of the Charring Material Ablation (CMA) code and preserves the basic features of CMA. Only the modifications to the CMA input-output procedure are detailed here; therefore, this manual should be used in conjunction with the CMA user's manual (Reference 5).

The major modification to CMA is the inclusion of erosion in the recession calculations. CMAE contains an erosion model, developed in the Particle Impact Erosion program, for the subsonic-transonic regions of rocket nozzles. Details of the model development are given in Reference 1. In summary, the erosion model contains two components: mechanical erosion due to mechanical mass removal of material, and chemical erosion due to chemical reactions between molten particles and the surface. Each erosion component is in the form of a G-law, G being the ratio of mass flux of target material removed to mass flux of particles incident upon the surface. G is related to particle impact conditions in the form of power laws commonly used in reentry vehicle erosion research (Reference 11).

Following sections briefly describe the CFC and CMAE codes and the changes to the SPP and CMA user's manuals required to use them. Sample cases executed with CFC and CMAE are also presented.

PART 1

CHAMBER FLOWFIELD CODE (CFC)

PREVIOUS PAGE IS BLANK

SECTION 2

CFC ANALYTICAL BASIS

Particle impact conditions can be determined if the particle trajectories within the nozzle are known. Since the particle and gas phases affect one another, a coupled two-phase flowfield calculation must be made to establish the particle trajectories. The coupled calculation must also account for other important nozzle flow characteristics, such as compressibility, two-dimensional (axisymmetric) flow, and the presence of different sized particles within the nozzle. Additionally, since the particle trajectories in the entrance region are expected to be strongly influenced by the chamber and grain geometry, the flow calculation must include most, if not all, of the chamber region, as well as the nozzle entrance and throat regions. To achieve these requirements in the CFC, three major changes were made to the FCT code:

- Extension of the calculation domain to include the chamber
- Modification of inflow boundary conditions to account for mass injection from the propellant grain
- Modification to particle trajectory calculations to evaluate trajectory crossovers and particle impact at the wall

All changes were made to existing subroutines; no new subroutines were added. The changes are discussed in the subsection below, where it is

PREVIOUS PAGE IS BLANK

assumed that the reader is well acquainted with the FCT module of SPP and its documentation (Reference 4).

2.1 GEOMETRY

The calculation domain of the base (FCT) code includes only the nozzle entrance and throat regions. The starting line for the calculations is a fictitious inflow boundary drawn in the vicinity of the nozzle inlet. Since the effect of the chamber and grain geometry is expected to be significant on particle impact conditions, the calculation domain was extended into the chamber.

The FCT code uses an algebraic procedure to generate a finite difference grid in the interior, given the distribution of mesh points along the boundaries. The procedure follows the transformation credited to Coons (Reference 6) and described by Cook (Reference 7). The transformation achieves uniform spacing of the mesh grid in the computation (x-y) space, but in general results in a nonuniform, nonorthogonal mesh in the physical (z-r) space.

There were a number of ways in which the mesh generator used in FCT could be extended to include the chamber. The options considered for this task are shown in Figure 1 along with the relative advantages and disadvantages of each. Generally, extension of the mesh into the chamber results in poor orientation in some part of the flowfield since the algebraic generator does not control the direction of the mesh lines, except those coincident with the boundary. An alternative is to use an elliptic solver which controls both the spacing and the direction of the mesh lines at and near the boundaries. However, adapting an existing elliptic solver to this problem would have required more resources than were available in this program. Hence, the algebraic mesh generation procedure used in FCT was

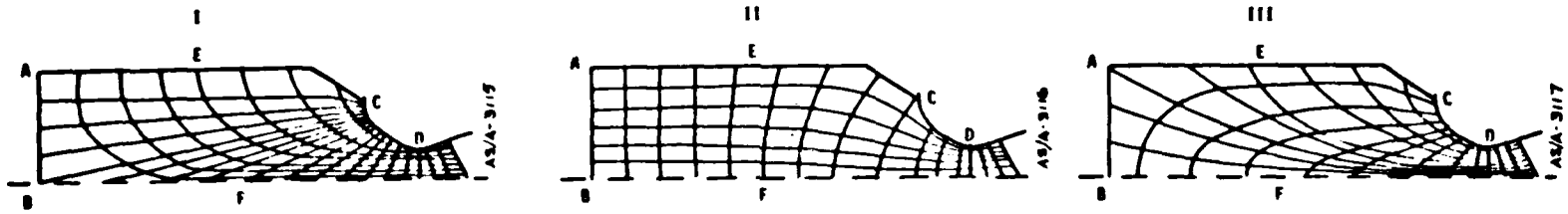

- Good mesh orientation near C and along $\overline{CD}$
- Good orientation along $\overline{AC}$
- Must change front end calculation
- Poor orientation around B and along $\overline{BF}$
- Retains current mesh distribution along $\overline{CD}$

- Good orientation around A and B
- Poor orientation around C
- Required integrating mesh distribution along $\overline{AEC}$ with distribution along $\overline{CD}$

- Good orientation around C and along $\overline{CD}$
- Good orientation around B and along $\overline{AB}$
- Poor orientation along $\overline{AE}$
- Retains current mesh distribution along $\overline{CD}$, outflow symmetry axis
- Minimum modifications to main body of FCT element

Figure 1. Mesh Generation Options

retained for CFC. Moreover, the third option shown in Figure 1 was selected because it yields a good mesh orientation in the primary region of interest, i.e., in the vicinity of the nozzle wall.

The chamber geometry is input to CFC by specifying the radial and axial coordinates of various points along the boundary. There are provisions in CFC to indicate the presence of a front end closure so that the boundary conditions there are treated differently. The algebraic mesh generator cannot handle submerged geometries. Hence, a computational boundary must be drawn spanning the submerged region. The code normally distributes mesh points uniformly with the wetted length along the chamber and grain boundary. If the presence of a front end closure or a submerged region inflow boundary is indicated, the code allows the specification of a minimum number of mesh points along the boundaries of each of these regions.

The patch line separating Regions I and II (cf., Reference 4) is also input by the user in CFC by specifying the coordinates along the line. This gives the user some control over the mesh generation in the interior region of the chamber and nozzle. Except for the new features noted above, the mesh generation procedure in the new code remains unchanged from that in in FCT.

As in FCT, only axisymmetric geometries are allowed by the new code. However, nonaxisymmetric configurations such as star shaped or axially slotted grains can be handled by approximating them with equivalent axisymmetric geometries. The procedure to determine the equivalent geometries is explained in detail in Section 5.

2.2 BOUNDARY CONDITIONS IN THE CHAMBER

The gas flow boundary calculations in CFC have been modified to handle the mass injection conditions at the grain and other inflow surfaces. The code can also account for the conditions at a chamber front end closure with no mass injection. These two types of boundary conditions are described below.

Inflow Boundary Conditions

The inflow boundary conditions are specified in CFC by inputting a grain burn-rate law or mass flux distribution along the inflow surface. The burn-rate law used in CFC has the form:

$$\dot{m} = cp^b \tag{1}$$

where

$\dot{m}$ is the gas* mass flux across the boundary

p is the static pressure

and

b, and c are constants for a given location

The values of b and c may vary with location along the boundary. The burn-rate law can also be used to specify the mass flux along any portion of the boundary by setting b = 0 in that region. The mass flux distribution is then input through c.

---

*The input procedure in CFC calls for the burn-rate law to be specified in terms of total mass flux (gas and particles). Since the particle to gas mass ratio is also input, the code internally adjusts the constant, c, to account for the proportion of gas flow at the inflow boundary.

The burn-rate law replaces the isentropic relation for pressure used in FCT at the inflow boundary. The five equations used to solve for the flow conditions at the inflow boundary are:

- Compatibility equation along the negative branch of the characteristic curve in the x-t plane*
- Energy equation (in the form of an adiabatic flow relation for temperature)
- Equation of state
- Gas inflow direction
- Burn-rate law

The form of the first four equations remains unchanged from that in FCT. The form of the final equation is derived below. Starting from the general mass flux relation:

$$\dot{m} = \rho \vec{V} \cdot \vec{n}$$

we have

$$\dot{m} = \rho \frac{2\pi r(udr - vdz)}{2\pi r \sqrt{dr^2 + dz^2}} \qquad (2)$$

where ρ is the gas density, $\vec{n}$ is a unit vector normal to the surface, and $\vec{V}$ is the gas velocity vector with components u and v in the axial (z) and radial (r) directions, respectively. A sketch showing the velocity

---

*x is a transformed coordinate which is zero along the inflow plane and one at the outflow plane; t refers to time (see Reference 4).

components and defining the wall angle, β, and gas flow angle, α, is shown below:

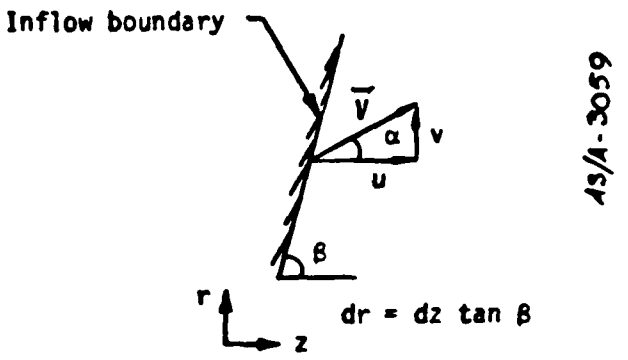

Combining Equations (1) and (2) with the relation between velocity components and the perfect gas law, we have:

$$u = \frac{c}{A_u} R_g \, p^{b-1} T \tag{3a}$$

$$v = \frac{c}{A_v} R_g \, p^{b-1} T \tag{3b}$$

where

$$A_u = \sin \beta \, (1 - \tan \alpha \cot \beta) \tag{4a}$$

$$A_v = \cos \beta \, (\cot \alpha \tan \beta - 1) \tag{4b}$$

R_g is the gas constant and T is the gas temperature.

The velocity components given by Equations (3a) and (3b) satisfy the relation:

$$v = u \tan \alpha \tag{5}$$

Note that in CFC, in the absence of user input specification to the contrary, the gas flow angle is assumed perpendicular to the inflow surface.

The two-step procedure used in FCT to calculate the flow conditions at the boundaries is maintained in CFC. Within each step the five governing equations mentioned earlier are solved by iteration for u, v, p, T and ρ. The convergence criterion for the iteration calculations is based on pressure. Convergence occurs usually within two to three iterations.

No Mass-Injection Boundary Condition

A surface with no mass injection in the chamber cannot be reduced to a special case of the grain burn-rate law condition described above. Since such boundary conditions are often encountered at the front end of the chamber, CFC is written to handle that region separately, if required. If the user signals the existence of a zero mass-injection front end region in the chamber geometry input, a separate set of equations are solved by the code. Five equations are again required to solve for the five unknowns (u, v, p, T and ρ), except at the center (axis) point which is treated as a stagnation point with $u = v = 0$. At all points on the front end closure, except for the stagnation point, the five equations used to solve for the flow conditions are:

1. Compatibility equation along the negative branch of the characteristic curve in the x-t plane
2. Energy equation (along a streamline)

3. Equation of state

4. Flow-surface tangency (slip) condition

5. Compatibility equation along the negative branch of the characteristic curve in the y-t plane*

The first and third conditions remain unchanged from before. The fourth condition is satisfied by making the flow angle equal to the wall angle. Hence,

$$v = u \tan \beta \tag{6}$$

The remaining two conditions are obtained from the characteristic compatibility equations in the y-t plane. The fifth condition is obtained along the negative branch of the characteristic curve, namely:

$$\frac{dy}{dt} = \bar{v} - a\delta \tag{7}$$

The negative (left running) characteristic is used since it is assumed that the flow direction is from the grain to the axis. The compatibility equation along that characteristic is given by:

$$\frac{dp}{dt} - \frac{\rho a}{\delta} y_z \frac{du}{dt} - \frac{\rho a}{\delta} y_r \frac{dv}{dt} = a^2 R_1 - \frac{\rho a}{\delta} y_z R_2 - \frac{\rho a}{\delta} y_r R_3 + R_4 \tag{8}$$

where

$$\bar{v} = u\, y_z + v\, y_r \tag{9}$$

---

*y is the transformed coordinate which is zero along the axis and one along the nozzle wall (see Reference 4).

and

$$\delta = \sqrt{y_z^2 + y_r^2} \tag{10}$$

The subscripts z and r refer to the partial derivatives in those directions. The term a is the local sound velocity. The variables $R1$, R_2, R_3 and R_4 in Equation (8) are the inhomogeneous terms in the continuity, x-direction momentum, y-direction momentum and energy equations, respectively, written for the y-t reference plane. The Equations (7) through (10) are from Reference 4 and can be derived using the methods of Reference 8.

Equation (8) is written in partial differential form* as:

$$(p_t + \lambda_- p_y) - \frac{\rho a}{\delta} y_z (u_t + \lambda_- u_y) - \frac{\rho a}{\delta} y_r (v_t + \lambda_- v_y) = R_- \tag{11}$$

where λ_- = dy/dt, given by Equation (7), and R_- is the right hand side of Equation (8). The negative subscripts signify that these terms are written for the negative characteristic branch.

Casting Equation (11) in one-sided difference form, we have:

$$\left(\frac{p_3 - p_1}{\Delta t} + \lambda_- \frac{p_6 - p_1}{\Delta y}\right) - \frac{\rho a}{\delta} y_z \left(\frac{u_3 - u_1}{\Delta t} + \lambda_- \frac{u_6 - u_1}{\Delta y}\right) - \frac{\rho a}{\delta} y_r \left(\frac{v_3 - v_1}{\Delta t} + \lambda_- \frac{v_6 - v_1}{\Delta y}\right) = R_- \tag{12}$$

---

*Note that this procedure represents a departure from the method used to transform the corresponding equation in the x-t plane, where the ordinary differential of the compatibility equation along the characteristic was cast in difference form.

where the subscripts 1, 3 and 6 refer to the points shown in the sketch below:

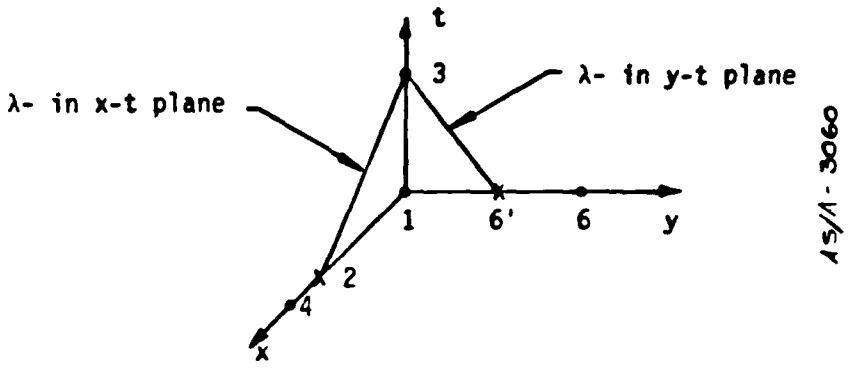

The point 3 is at the new time where the flow conditions are to be evaluated. Points 1 and 6 lie in the same y-t plane as point 3, but at an earlier time where the conditions are known. Information about these conditions are transmitted to point 3 via the characteristic in the y-t plane shown. The situation is similar to that in the x-t plane where information is transmitted from point 2 to point 3 via the indicated characteristic. However, since the formulation of the difference equation in the y-t plane was obtained from the partial differential form, the conditions at point 6' do not enter the equation explicitly. Hence, the precise location of the intersection of the characteristic curve in the y-t plane with the y-axis, i.e., point 6', does not have to be evaluated.

The remaining condition (condition 2) is obtained from the energy equation along the streamline, that is:

$$\frac{dp}{dt} - a^2 \frac{d\rho}{dt} = R_4 \tag{13}$$

and

$$\lambda = \frac{dy}{dt} = \overline{v} \tag{14}$$

Again, writing Equation (13) in partial differential form, we have:

$$(p_t + \lambda p_y) - a^2 (\rho_t + \lambda \rho_y) = R_4 \tag{15}$$

which when written in one-sided difference form about point 1 in the y-t plane, gives:

$$\frac{p_3 - p_1}{\Delta t} + \lambda \frac{p_6 - p_1}{\Delta y} - a^2 \left(\frac{\rho_3 - \rho_1}{\Delta t} + \lambda \frac{\rho_6 - \rho_1}{\Delta y} \right) = R_4 \tag{16}$$

Equations (6), (12) and (16) were incorporated into the new code. The equations for the other two conditions (compatibility equation in the x-t plane, and the equation of state) remained unchanged from the base code. This set of equations are solved iteratively at the points along the boundary where the front end closure is specified. The convergence criterion is again based on pressure.

Finally, at the center of the front end closure, stagnation point conditions are imposed. Hence u and v are set to zero and Equations (6) and (12) are not required. The remaining three equations are solved iteratively for pressure, density and temperature, with the convergence based on pressure as before.

2.3 PARTICLE TRAJECTORY CALCULATIONS

Particle trajectory calculations were modified to calculate conditions resulting from trajectory cross-overs and wall impact. Changes were also made to the manner in which the particle size distribution is calculated. These changes are discussed below.

Particle Size Distribution

The base (FCT) code has a built-in empirical procedure for calculating the size distribution of aluminum oxide particles in the nozzle. However, for impact calculations in the entrance region, the large aluminum particles ejected from the grain are more important than the small aluminum oxide particles. The large particles are more likely to impact the nozzle walls since they cannot follow the gas stream very closely around the nozzle contour. Additionally, larger particles cause greater mass removal. Hence, a procedure to calculate the size distribution of aluminum particles in the chamber was incorporated into the new (CFC) code.

The procedure used was developed by Hermsen (Reference 4) for use in the combustion efficiency calculations of the Solid Performance Program (SPP). The procedure is not accessible from the FCT module of SPP. Hence, it was added to the transonic calculation procedure in CFC. The average size of aluminum particles coming off the propellant grain is correlated with the grain burnrate and the percentage of ammonium perchlorate in the propellant. The distribution of particle sizes about the mean is assumed to be log-normal, with an empirically determined value of the standard deviation.

Presently, the Chamber Flowfield Code does not account for changes in the aluminum particle size distribution due to combustion or breakup. Since most of the breakup occurs in the throat region and since rough calculations indicate that there are still large unburnt particles at the entrance to the

nozzle, this approximation is reasonable for obtaining estimates of the impact condition in the nozzle entrance region.

Trajectory Crossovers

The two-phase flow in FCT is calculated using a hybrid procedure which appears to be quasi-steady but which actually yields a fully coupled solution. The gas phase equations are integrated in a time dependent form, while the particle phase equations are integrated in a steady state form. The gas phase calculations are allowed to relax for a given number of time steps before a particle phase calculation is performed. The gas calculations define the flowfield for determining the aerodynamic forces on the particles. The particle calculations in turn determine the gas-particle coupling terms used in the next set of gas phase calculation . The particle phase calculations are performed by tracing the trajectories of individual particles from selected points on the inflow boundary using a force-momentum balance on the particles. The particle trajectories are then treated as particle streamlines. The spatial density of particles is calculated knowing the particle mass flowrate, the average velocity, and the spacing between adjacent streamlines. The spatial density is important in calculating the coupling terms and impact conditions.

This hybrid procedure to calculate the coupled gas-particle flow was maintained in the new (CFC) code. However, since particle trajectories in CFC start from the chamber, they often intersect each other. Trajectory crossovers may also occur if particles cross the centerline, or if they impact the nozzle wall. In the FCT code it is assumed that these trajectory crossovers do not occur; therefore, the new code required modifications to account for the crossovers so particle spatial densities could be calculated correctly with the total mass flowrate of particles being conserved.

The particle mass flowrate between adjacent streamlines is determined at the inflow boundaries by calculating the gas flowrate between adjacent trajectory initiation points, and multiplying by the overall particle to gas mass ratio. This particle mass flowrate associated with each pair of streamlines remains unchanged until crossover or impact occurs. When crossover occurs, new pairs of adjacent streamlines are formed and the mass flowrate between them must be reassigned. An example of how this is accomplished in CFC is explained with reference to the sketch below:

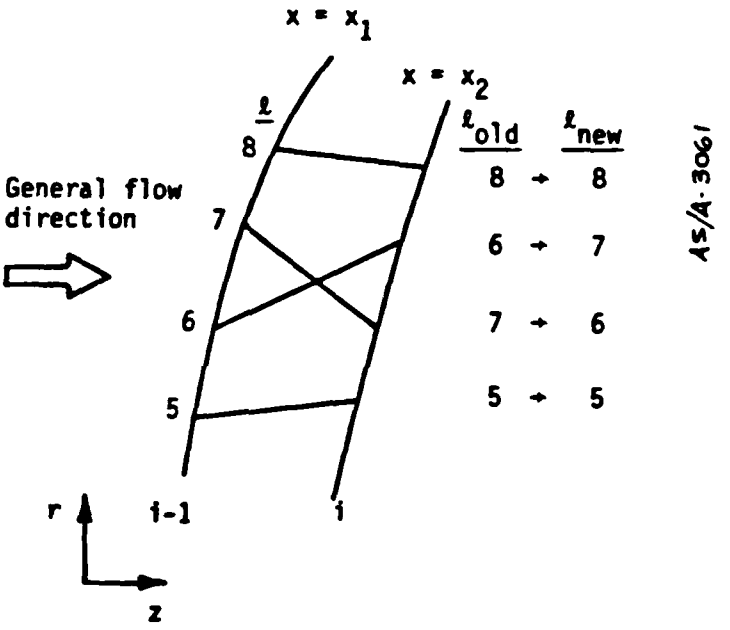

The sketch shows the particle trajectories between two neighboring axial* stations. The particle densities are calculated at the mesh points in the code; hence, the mass flowrate between the particle streamlines at each axial station must be known. At each of those stations, the particle

*In the transformed coordinates. Hence, axial stations in this context refers to constant x mesh lines.

trajectory indentifier (index ℓ), is renumbered starting from the bottom. The code searches for changes in the numbering sequence to indicate the presence of particle crossover. If particle crossover is detected, the mass flow between the streamlines is reassigned. In going from one axial station to the next (say from the line with index i-1 to the one with index i), it is assumed that the particles are confined between initially adjacent streamlines. This is shown schematically below for each of the three pairs of streamlines of the earlier sketch.

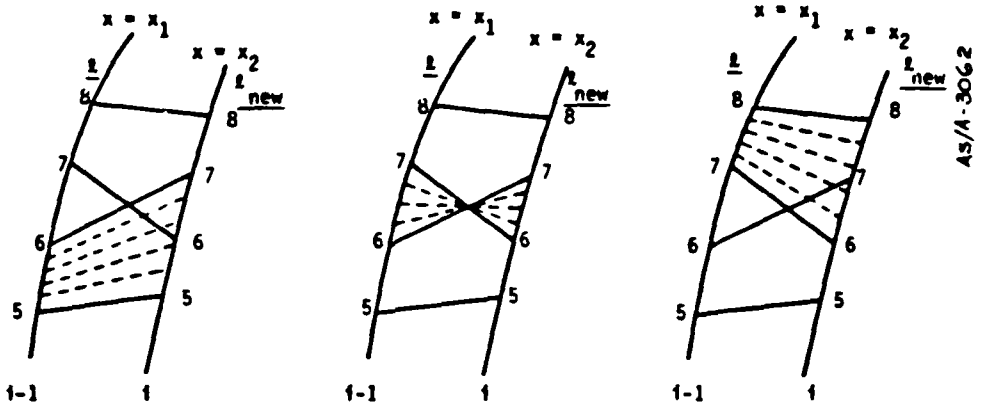

Note that the region between streamlines 6 and 7 at i gets contributions from all the three flow areas shown at i-1. Also, the particle mass flowrate confined between streamlines 5 and 6 at i-1 is distributed between the pairs 5-6 and 6-7 at i. A similar situation occurs for the streamline pair 7-8 at i-1. In some cases, when a streamline intersects more than one other streamline, the mass between one pair of streamlines at one axial station may be spread over a number of pairs at the next axial station. The distribution of mass at the new location is based on the assumption that the particle spatial density between adjacent streamlines is uniform along a line of constant x. The mass flowrate between two streamlines, $\Delta\dot{m}_p$, is therefore proportional to the dot product of the average particle velocity

vector, $\vec{V}_p$, and the area vector, $\overrightarrow{\Delta A}$, at the new axial station. For example, to determine the flowrate between streamlines 5 and 6 at i, we have:

$$\Delta\dot{m}_{p(5-6)i} \sim (\vec{V}_p \cdot \overrightarrow{\Delta A})_{(5-6)i} \tag{17}$$

also

$$\Delta\dot{m}_{p(5-6)i-1} = \Delta\dot{m}_{p(5-6)i} + \Delta\dot{m}_{p(6-7)i} \tag{18}$$

and

$$\Delta\dot{m}_{p(6-7)i} \sim (\vec{V}_p \cdot \overrightarrow{\Delta A})_{(6-7)i} \tag{19}$$

Hence,

$$\Delta\dot{m}_{p(5-6)i} = \Delta\dot{m}_{p(5-6)i-1} \frac{(\vec{V}_p \cdot \overrightarrow{\Delta A})_{(5-6)i}}{(\vec{V}_p \cdot \overrightarrow{\Delta A})_{(5-6)i} + (\vec{V}_p \cdot \overrightarrow{\Delta A})_{(6-7)i}} \tag{20}$$

A similar expression can be derived for the flowrate between streamlines 7 and 8 at i. However, the flowrate between streamlines 6 and 7 at i must account for incoming particles from three flow areas at i-1. In that case, we have:

$$\Delta\dot{m}_{p(6-7)i} = \Delta\dot{m}_{p(6-7)i-1} + \Delta\dot{m}_{p(5-6)i-1} \frac{(\vec{V}_p \cdot \overrightarrow{\Delta A})_{(6-7)i}}{(\vec{V}_p \cdot \overrightarrow{\Delta A})_{(5-6)i} + (\vec{V}_p \cdot \overrightarrow{\Delta A})_{(6-7)i}}$$

$$+ \Delta\dot{m}_{p(7-8)i-1} \frac{(\vec{V}_p \cdot \overrightarrow{\Delta A})_{(6-7)i}}{(\vec{V}_p \cdot \overrightarrow{\Delta A})_{(6-7)i} + (\vec{V}_p \cdot \overrightarrow{\Delta A})_{(7-8)i}} \tag{21}$$

Note that this procedure conserves the particle mass flow through the nozzle.

The procedure for reassigning mass flow between particle streamlines is executed within the code whenever particle crossover is detected at or just prior to a given axial station. When no crossover occurs, the mass flow between adjacent streamlines remains unchanged between subsequent x mesh locations.

A different type of a crossover occurs when a particle trajectory intersects the centerline. Since there is always a particle streamline at the centerline, there is a trajectory crossover, but this particular case is handled differently in the code. When a particle approaches the centerline, the code reflects it off the axis in real space, as shown in the sketch below.

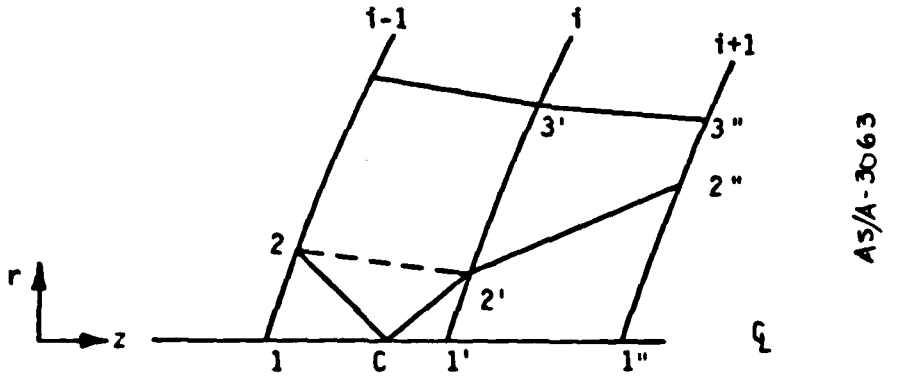

When streamline 2 reaches the axis at C it is reflected to point 2' on the ith x mesh line. In the real flow case this corresponds to the streamline at 2 passing down through the centerline at C, and another streamline from the opposite side emerging from the centerline at the same location (symmetric flow assumption). However, in calculating the particle spatial density at the x mesh lines, the code assumes the particle streamline goes directly from 2 at

i-1 to 2' at i, as shown by the dashed line. Hence, there is no need to reassign the mass flowrate between the streamlines.

Note that although the spatial density calculations make the assumption that the particle streamlines goes directly from 2 to 2', the particle trajectory calculations do not. That is, the portion of the trajectory 2 between i and i+1 (the straight line 2'-2") is an extension from the solid line C-2', not the dashed line 2-2'.

Wall Impact

The base (FCT) code does not allow particles to impact the wall. When particles get very close to the wall they are forced to move parallel to the wall. Since wall impact prediction is the primary objective of this analytical procedure, the restriction against wall impact was removed in the new (CFC) code. Further, the mass deposited on the walls and the conditions of impact are calculated.

The mass of particles reaching the wall are calculated using a procedure similar to that used in distributing the mass flow after trajectory crossover. The location of impact is calculated and stored by the code. When the code begins to calculate mass flow between streamline and particle spatial densities, it checks for wall impact (in addition to trajectory crossover) from one axial station to another. If impact is detected, the particle mass flowrate reaching the wall is calculated. It is assumed that the mass of particles reaching the wall is removed from the flow.

The procedure for calculating the mass of particles reaching the wall is described with reference to the example shown in the sketch below. The particle streamline 10 impacts the nozzle wall at point P between the axial stations i-1 and i. The mass flowrate between the streamlines 9 and 10 at i-1 is divided into two parts: some of the mass is deposited on the wall between

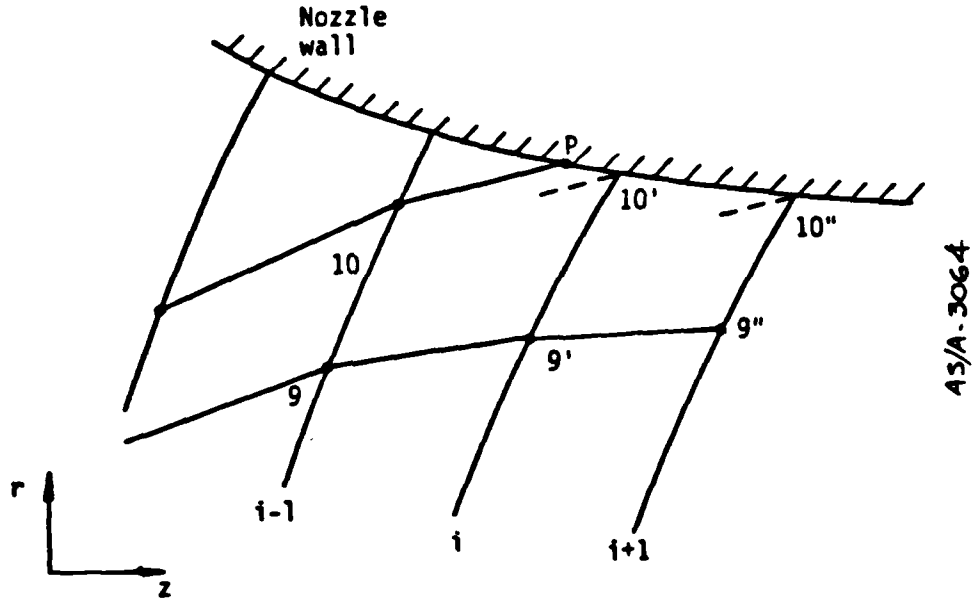

P and 10' and the remainder passes through the points 9' and 10'. (The point 10' is where the axial station i intersects the nozzle wall). The distribution of mass is again taken proportional to the values of the vector dot product $\vec{V_p} \cdot \vec{dA}$ between P and 10' and between 9' and 10'. The vector dot product is based on the average velocity in the region of interest. The average velocity is obtained by taking the arithmetic mean of the velocity components at the regions' extremities. In this case, the velocity at point 10' is not known. It is assumed to be the same as point P since the two points are generally located very close to one another.

The procedure is then repeated at the next axial station. The mass flow through 9' and 10' at i is partly deposited at the wall between the points 10' and 10", while the rest flows through the region between the points 9" and 10". Note that at each of the downstream x-mesh wall points 10', 10", etc., there is a remnant of the original streamline 10. The procedure continues at subsequent axial stations until another streamline

impacts the wall or the remnant streamline breaks free from the wall. The latter occurs when the wall curves away sufficiently that the remnant velocity vector is no longer pointing into the nozzle wall. Once a streamline breaks free from the wall, it is treated as any other streamline in the flow, with the mass between it and the adjacent streamline reduced to account for mass deposition upstream of the breakaway point.

As mentioned earlier, the code calculates impact conditions as well as the impact location. The quantities required for calculating erosion due to particulate impact, such as particle velocity, mass flux and impact angle, are calculated and printed in the output for each particle size group. The particle size group gives the remaining parameter required for calculating erosion, that is, particle size. The impact conditions are then used as input to the ablation-erosion code which is discussed in Part 2.

P. 36 BLANK

SECTION 3

CFC OVERALL STRUCTURE

The Chamber Flowfield Code (CFC) is structured as a stand-alone version of the Fully Coupled Transonic (FCT) module of the Solid Performance Program (SPP). Figure 2 shows a comparison between the overall structures of SPP and CFC. The control module in CFC serves only to read in the variables in the SPP namelist required for CFC, and call the TD2P module which in turn executes the modified FCT.

The input data requirements for CFC are given in Table 1. A brief description of each input is also given, and sections containing greater detail are identified. The input data set for CFC contains fewer items than the complete set for SPP. However, note that there is a new namelist, called TD3, where the new input variables required for the modified version of FCT are specified.

Since CFC does not contain thermochemical expansion or ballistics modules, the variables transmitted in SPP from these modules to, and used by, FCT must now be specified in the TD2 namelist. The only variable transmitted from the ballistics module is the chamber pressure. This can be obtained from a test firing pressure trace, if available, or by running a ballistics code, such as the BAL module of SPP. The thermochemical variables can be obtained by running an equilibrium expansion code, such as the One-Dimensional

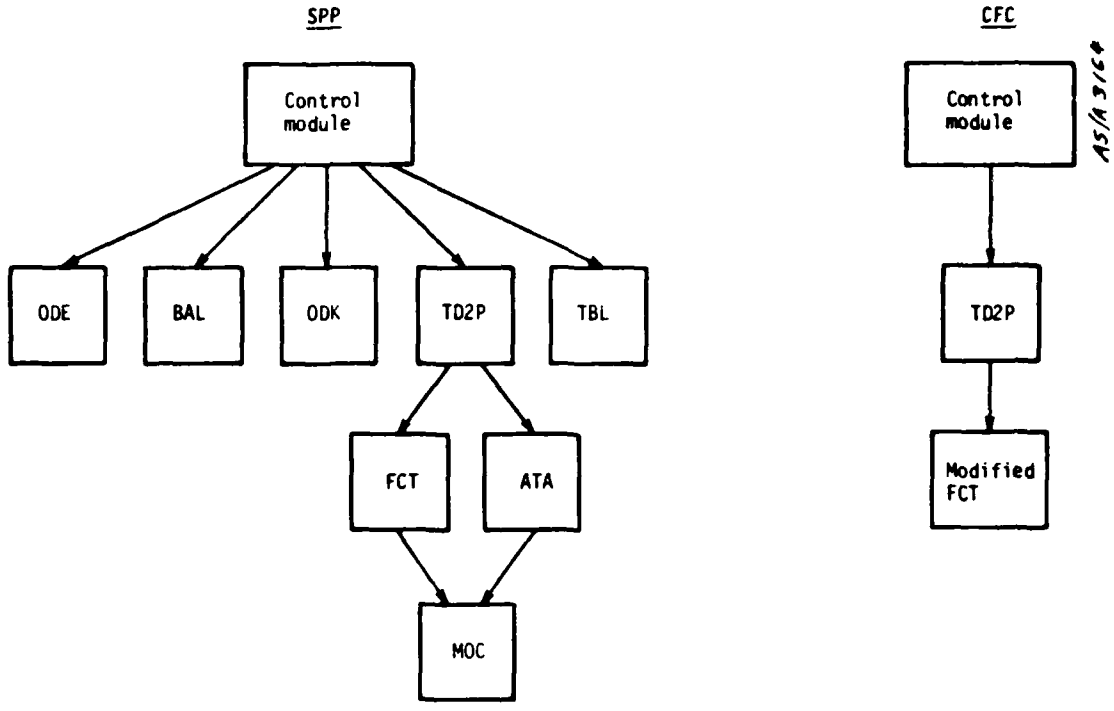

Figure 2. Comparison of Overall Structures of SPP and CFC

Table 1. Input Data Set Description

Card Input	Description	Section No.
T I T L E : }	One or more title cards	4.0
S P P	SPP directive card	4.0
$ S P P : $ E N D	SPP namelist for nozzle geometry and computer plotting	4.1
$ T D 2 : $ E N D	TD2 namelist for old FCT variables	4.2
$ T D 3 : $ E N D	TD3 namelist for new FCT variables	5.0

Equilibrium (ODE) module of SPP or the Aerotherm Chemical Equilibrium (ACE) code (Reference 9). An example of how an ACE expansion is utilized for CFC input is shown in the discussion of the sample case (Section 7).

SECTION 4

SPP INPUT CHANGES FOR CFC

This section describes changes to the existing SPP input variables required to execute CFC. Essentially the input is set up as if FCT alone were to be run on SPP. Of all the data required by the SPP code, only the SPP directive card and the SPP and TD2 namelists are, therefore, required. Title cards may be input, if desired. The formats for the title cards, the SPP directive card and the two namelists are the same as in SPP. However, the namelist data requirements are simplified because only the modified FCT module is executed, and since specific impulse calculations are bypassed.

4.1 SPP NAMELIST

The function of the SPP namelist in CFC is to input the nozzle wall geometry and computer plotting variables. Changes to the namelist are described below under the same headings used in the SPP user's manual (Reference 4).

Modules to be Executed, Etc.

TD2P = 1.

This is presently the only acceptable specification. Calls to other modules have been eliminated.

ODK Start Option

Not required.

PREVIOUS PAGE IS BLANK

Missile Trajectory

Not required.

Nozzle Geometry

Specify the following:

RSI

Nozzle Inlet Geometry (INLET and corresponding geometry variables)

Nozzle Exhaust Geometry (IWALL and corresponding geometry variables)

Note: Although CFC calculations extend only up to the nozzle attachment point, a cone or contour geometry beyond that location must be specified. The geometry beyond the attachment point may be fictitious since it will not affect the calculations.

Nozzle Throat-Erosion Data

Not required.

Combustion Efficiency Calculations

Not required. Calculation of aluminum agglomerate sizes using the internal empirical correlation is available as an option in the TD3 namelist.

Computer Plotting

FCT plots only. Specify PLTT, PRNTPL and FCT plot variables.

Note: No changes have been made to the SPP plot routines. The code, as received, does not save plots. Although the plots are not saved, both the NPLTS and NSPLTS vectors must be specified for generating plots during a run. Set NSPLTS = NPLTS.

4.2 TD2 NAMELIST

Changes to the TD2 namelist are described under the same headings as used in the SPP user's manual.

Items Communicated for ODE and BAL Modules

All items must be specified. In addition, CPS, the solid particle heat capacity in ft^2/sec^2 °R should be included in the namelist.

The default value of XMLW, the molecular weight of the condensed phase, has been changed to that for aluminum (26.98154 lb/lbmole).

Perfect Gas Option

If the perfect gas option is desired (PGFLG is set equal to 1.), GAMMA and CPG must be specified.

Particle Data

The five options for calculating aluminum oxide particle group sizes in SPP are still in effect in CFC. However, the default values of some of the variables have been changed to facilitate aluminum agglomerate particle group size calculations. Options 4 and 5 in SPP can also be used in CFC to directly input aluminum particle sizes and distributions. In addition, a sixth option has been added to calculate the mean aluminum particle size via an empirical correlation. These options are discussed below.

Option 4: Input of DPBAR

In this option a mean particle diameter, DPBAR, is input. If the number of particle groups requested is more than one, the particle group sizes are automatically calculated using a log normal distribution. The number of particle groups desired is input through the variable NPG, and the geometric standard deviation of the log normal distribution is input through SIG. As in SPP, the particle mass fractions are distributed uniformly over all size groups.

Option 5: Input of R and WPWT

In this option the size of the particle groups are input through the R array, and the corresponding weight fractions of each group are input through the WPWT array.

Option 6: Input of RDOT and ALFAAP (in TD3 namelist)

This is the recommended option. Here the mean particle diameter, DPBAR, is not input but calculated using Hermsen's correlation for mean aluminum agglomerate size. This correlation, which is also used for combustion efficiency calculations in SPP, relates DPBAR to the grain burn rate (RDOT) and to the mass fraction of ammonium perchlorate in the propellant (ALFAAP) as follows:

DPBAR = 35.0/RDOT/ALFAAP

The particle size groups are then calculated using the log normal distribution. Hermsen characterizes the aluminum agglomerate size distribution by a standard deviation of $\log_{10}D$ equal to 0.2. The default value of SIG was selected to be consistent with this empirically determined value.*

Options 4 Through 6

In addition to the variables mentioned above, the particle material density is required. It can be in terms of the variable SMP if the material densities of all particle groups can be considered equal and invariant with temperature. Later, an array variable ROPMK is described which allows for the specification of density as a function of particle group and temperature.

---

*SIG is related to σ_a, the standard deviation of $\log_{10}D$, as follows:

SIG = 10^{σ_a}

The code will assume a default value of 147.6 lbm/ft^3 (density of liquid aluminum), if SMP or ROPMK are not specified in the TD2 namelist.

The input variables for options 4 through 6 are summarized below:

Option	Item	Description	Units	Default Value
4,6	NPG	Number of particle groups to be considered. NPG must be less than or equal to 5.	None	3
4 to 6	SMP	Particle material density	lbm/ft^3	147.6
4	DPBAR	Mean particle diameter	m	0.0
4,6	SIG	Geometric standard deviation for log normal particle size distribution	None	1.585
5	R(1)	Array of particle radii. Maximum of 5. Must be input in ascending order. Add a zero to the list after the final (maximum) value to indicate end of set.	ft	0.0
5	WPWT(1)	Particle weight flow fractions corresponding to each of the above particle radii. Entries must add to one.	None	--
6	RDOT	Propellant burning rate (input in TD3 namelist)	in./sec	0.0
6	ALFAAP	Mass fraction of ammonium perchlorate in propellant (input in TD3 namelist)	None	0.0

NOTE

If DPBAR is specified (other than zero), Option 4 will be executed and inputs of R(1) or RDOT and ALFAAP, if any, will be overridden. Also, an input of R(1) will execute Option 5 only if DPBAR is zero, regardless of RDOT and ALFAAP values. Finally, to execute Option 6, both RDOT and ALFAAP must be different from zero, and DPBAR and R(1) must both be zero.

Transonic Analysis Input Data

The input data used in CFC are given below:

Item		Description	Units	Default Value
FCT	=	.TRUE. The user has no discretion over this input. The Advanced Transonic Analysis (ATA) option is not available in CFC	logical	.TRUE.
RDPMK(1,K) 147.6		Particle material density table for the K^{th} particle group	lbm/ft^3	
TROMK (1,K) 0.0		Temperature table corresponding to the particle density table	°R	
NROM (K)		Number of entries in the ROPMK (1,K) TRDMK (1,K) tables. NROM (K) $\leq$ 10	none	0.0
NSMAX		Maximum number of time steps to be taken	none	1,000
NGIPI		Number of gas phase calculation steps per set of particle phase calculations	none	25

Print Control

Same as in SPP.

Time Step Control

Same as in SPP.

Mesh Generation Data

The inlet boundary and the patch line demarcating Regions I and II are input in the TD3 namelist. The only variables that need to be input in the TD2 namelist are: NX, NY, REG2, and ZMAXA. The description, units and default values of these variables are the same as in SPP. It is recommended that the variable REG2 be set to .TRUE. and the patch-line input as described in Section 5.

Inflow Boundary Condition Data

The gas-flow inlet boundary conditions are specified in terms of a grain-burn law or mass-flux distribution in the TD3 namelist. Hence, the option to specify any desired total pressure and temperature variation along the inflow boundary (via the vectors POIN and TOIN) is no longer applicable. The following options remain operational in the TD2 namelist for specifying the gas-phase boundary conditions:

ITHIN = flag controlling the distribution of the gas-phase flow angle along the inflow boundaries in the chamber

= -1 The flow angle is assumed normal to the inflow boundary (default option)

= 0 No longer applicable

= 1 The flow angles are input via the THIN array

If ITHIN is set equal to 1, the table THIN is specified in the same manner as in SPP. In this case, the vectors POIN(J) and TOIN(J) must be specified and set equal to 1.0. Note that in the default case (ITHIN = -1) the gas flow angle is assumed normal to the inflow boundary, which is a departure from the procedure used in SPP. The vectors POIN and TOIN need not be specified for the default option.

The data set for the particle phase boundary conditions remains the same as in SPP. The particle velocity is specified as a fraction of the gas phase velocity via the array PKK. The default value for PKK is 1. It is recommended that PKK be set equal to 0.2 to account for the velocity lag of the aluminum agglomerate at the propellant surface.

Remaining TD2 Data Sets

Not required.

SECTION 5

NEW INPUT VARIABLES FOR CFC

New input variables required for the Chamber Flowfield Code are read in through the namelist TD3. The new variables are related to changes in geometry, inflow boundary conditions and particle trajectory calculations. The data sets for these and other variables are described below.

Geometry

The chamber geometry is input in CFC by specifying the boundary coordinates RCHMB and ZCHMB, for the r and z directions, respectively. In general, the input coordinates describe the actual chamber and grain surface. However, in some cases they may define hypothetical computational inflow boundaries. For example, an axisymmetric approximation to the real boundaries must be employed for star-shaped, slotted, or other nonaxisymmetric grain configurations. The recommended procedure is as follows: at a given axial location, ZCHMB, an equivalent axisymmetric (circular) grain surface is defined with a port area equal to the actual axial flow area. The radius of the equivalent circular boundary is the radial coordinate, RCHMB, corresponding to ZCHMB. Figure 3 explains the details of the procedure. The mass injection rate must also be adjusted to account for the difference in surface areas between the real and computational boundaries. A perimeter adjustment

PREVIOUS PAGE IS BLANK

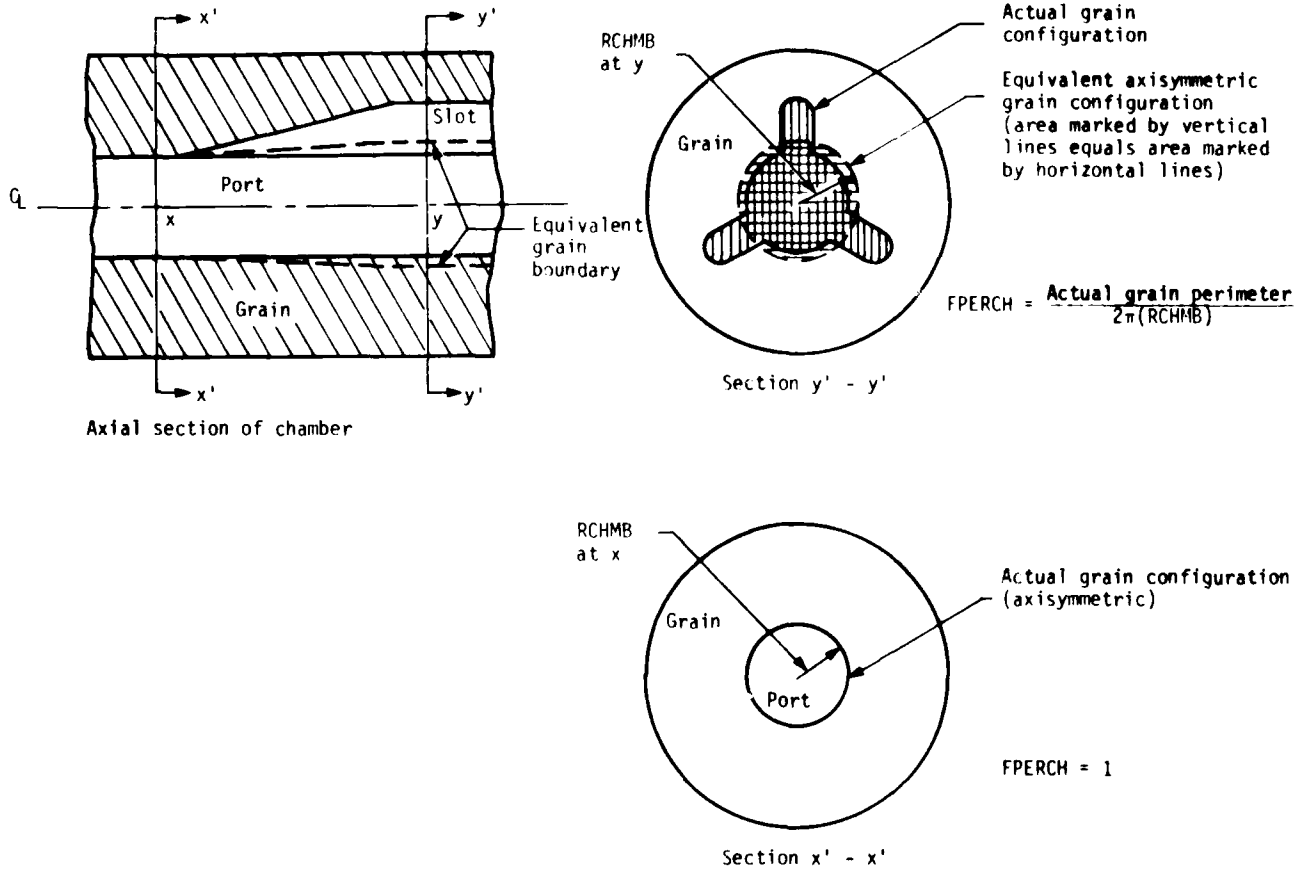

Figure 3. Axisymmetric Approximation of Non-Axisymmetric Grain Configurations

factor, FPERCH, is used for this purpose. As explained in Figure 3, FPERCH is the ratio of the real surface area to the computational boundary area at a given axial location.

The factor FPERCH may also be used in other regions of the chamber where the computational boundary does not correspond to the real boundary. For example, the current mesh generator has difficulty in mapping the submerged region. A computational boundary must therefore be drawn connecting the nosecap tangent point to some point on the grain surface, as shown by line DE in Figure 4. It is recommended that the line DE should not be at an angle greater than 60° to the nozzle axis. The factor FPERCH is then used to adjust the mass flow across the computational boundary DE so that it approximates the mass injected by the grain in the submerged region DF.

The chamber coordinates RCHMB and ZCHMB are input via two one-dimensional tables, similar to the nozzle wall coordinates specification. Likewise, the coordinates are normalized by throat radius, and the origin is at the center of the throat. The coordinates are specified starting from the front-end center of the chamber (point A in Figure 4). The last entry in the tables corresponds to the point where the chamber geometry meets the nozzle wall (point E in Figure 4). The total number of points input is specified by the variable ICHMB.

In many motor designs, the front end of the chamber has an impermeable boundary such as a solid wall; e.g., line AB in Figure 4. In that case the extent of the no-injection region must be specified so that the code treats that portion of the boundary separately, using slip-flow* instead of

---

*The point at the center of the front-end closure is treated as a stagnation point. Therefore, in the chamber geometry specification, the contour next to point A in Figure 4 should be normal to the wall.

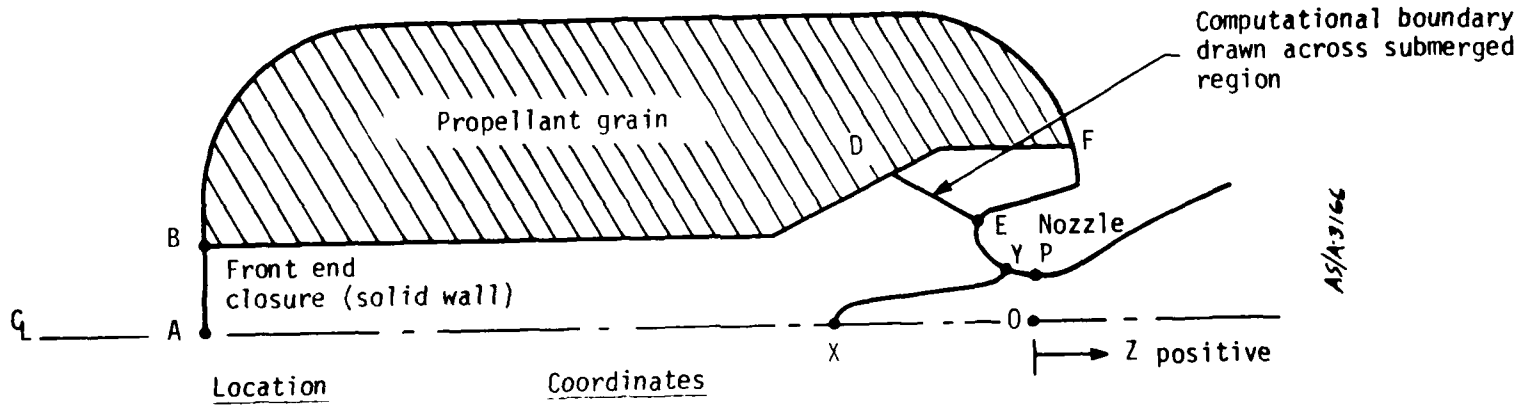

Location	Coordinates
A	RCHMB(1), ZCHMB(1); RCHMB(1) = 0.0
B	RCHMB(ICHMB1), ZCHMB(ICHMB1)
D	RCHMB(ICHMB2), ZCHMB(ICHMB2)
E	RCHMB(ICHMB), ZCHMB(ICHMB)

Origin is at point O

All dimensions are normalized by the distance OP (nozzle throat radius)

Figure 4. Chamber and Grain Configuration Schematic

mass-injection boundary conditions. This can be done by including the coordinates of the point demarcating the no-injection and mass-injection boundaries in the RCHMB and ZCHMB tables (point B in Figure 4). The point is then identified by specifying its position on the table via the variable ICHMB1. If a value of ICHMB1 is specified (other than 1), the code will automatically locate a mesh point at the demarcation point. The minimum number of mesh points in the no-injection region can also be input, if desired, by specifying the variable NYMIN1.

The extent of the imaginary boundary spanning the submerged region (line DE in Figure 4) can also be specified in a similar manner. The coordinates of point D are identified by specifying their array subscript, ICHMB2. A mesh point will then be automatically placed at D. The minimum number of mesh points along DE can also be input by specifying NYMIN2.

If Region II mesh generation is desired (REG2 = .TRUE. in the TD2 namelist), the user must also input normalized coordinates of the patch line separating Regions I and II. The patch coordinates are input via two one-dimentional arrays: RPATCH for the r coordinate, and ZPATCH for the z coordinate. The total number of coordinate pairs input is specified by the variable IPATCH.

Line XY in Figure 4 shows a typical patch line. The location of X and Y is such that the ratios of the lengths, OX/OA and PY/PE, are approximately equal. This ensures that the mesh spacing along the axis and the nozzle wall is approximately uniform in Regions I and II. Generally X and Y should be located such that the length ratios, OX/OA and PY/PE, are between one-quarter and one-half. Once the points X and Y are located, a smooth curve is drawn joining the two points. The curve should be roughly normal to the axis and the wall at points X and Y, respectively.

The table below summarizes the geometry variables input in the TD3 namelist.

Item	Description	Units	Default Value
RCHMB	table of normalized chamber (front-closure-grain-inflow boundaries) radial coordiates	non-dimen-sional	
ZCHMB	table of normalized chamber axial coordinates	non-dimen-sional	
ICHMB	number of entries in the RCHMB, ZCHMB tables. ICHMB $\leq$50	none	
ICHMB1	subscript of the chamber coordinates at the junction of a no-injection front end closure and a mass injection boundary	none	
ICHMB2	subscript of the chamber coordinates at the start of the imaginary inflow boundary across the submerged region	none	ICHMB
NYMIN1	minimum number of mesh points along the front-end closure boundary (NYMIN1 $\geq$2, if ICHMB1 >1)	none	3
NYMIN2	minimum number of mesh points along the imaginary boundary across the submerged region (NYMIN2 $\geq$2, if ICHMB2 < ICHMB)	none	2
RPATCH	table of normalized patch (line separating Regions I and II) radial coordinates	non-dimen-sional	
ZPATCH	table of normalized patch axial coordinates	non-dimen-sional	
IPATCH	number of entries in the RPATCH, ZPATCH tables. IPATCH $\leq$50	none	

Inflow Boundary Conditions

The inflow boundary conditions are specified in the form of a mass burn-rate law or mass flux distribution along a grain or other inflow surface. The burn-rate law has the expression:

$$\dot{m} = cp^b$$

where $\dot{m}$ is the mass flux in lbm/ft^2-sec

p is the pressure in psia

and b, c are constants at any given location.

The mass flux specification option is treated as a special case of the burn-rate law by setting the constant b equal to zero.

Since the constants b and c may vary along the grain and other inflow boundaries, they are input in tabular form via two one-dimensional arrays: BEXPCH for b and CBRNCH for c. The values of the constants are input in sequence corresponding to each point in the chamber coordinate tables; that is, BEXPCH (I) and CBRNCH (Z) are the values of b and c at the point RCHMB (I), ZCHMB (I). The values of the constants between two input points are calculated within the code by linear interpolation along the length of the chamber boundary.

The factor FPERCH (see the discussion under geometry) is also input in a one-dimensional array. The sequence of values in the FPERCH table corresponds to the sequence of points in the chamber coordinate tables. The code adjusts the mass injection rate, as calculated by the burn-rate law, by multiplying it by the corresponding value of FPERCH.

The inflow boundary conditions input in the TD3 namelist are summarized below.

Item	Description	Units	Default Value
BEXPCH	exponent b used in the grain burn-rate law	none	50 * 0.0
CBRNCH	constant c used in the grain burn-rate law	$\frac{bm/ft^2 - sec}{(psia)^b}$	50 * 1.0
FPERCH	ratio of actual to input surface areas	none	50 * 1.0

NOTE

The above three quantities are input in tabular form, with the values corresponding sequentially to the points in the chamber geometry coordinate tables.

Particle Size Calculation

If option 6 is selected for calculating the particle size groups, the values of RDOT and ALFAAP should be input (different from zero) in the TD3 namelist. See Section 3 for details.

Particle Streamline Starting Location Distribution

The distribution of the starting points of particle streamlines along the inflow boundary can be controlled by the user. The particle streamline starting locations are based on their particle mass flow fractions. Each streamline, L, has a given initial mass flow fraction, WPSCOL(L). The Lth streamline starts from a location such that the fraction of the total particle mass flow injected between it and the axis, along the inflow boundary, is equal to SPSCDL(L). The first particle streamline transverses the centerline; hence WPSCDL(1) = 0.0. Also the final streamline is a limiting streamline, hence WPSCDL(NIPPG) = 1.0, where NIPPG is the total number of streamlines (set equal to 10 in the code). The other values of WPSCDL(L) range between 0 and 1, arranged in ascending order of N.

The vector WPSCDL may be directly read in, if desired, in the TD3 namelist. Another available option is to let the code generate the distribution internally according to the relation:

$$WPSCDL(L) \cdot (L-1)^{WPEXP}$$

where the exponent WPEXP is an input constant. If the WPSCDL array is read in directly, WPEXP must be input equal to zero.

If the automatic WPSCDL generation option is used, the minimum number of streamlines starting from the submerged region (i.e., the imaginary inflow boundary spanning that region) can be specified. To use this feature, WPEXP must be specified other than zero, and ICHMB2 must be input to define the extent of the submerged inflow region. The minimum number of streamlines is then specified via the variable NPSSUB. NPSSUB is always greater than or equal to 2.

The variables used to define the particle streamline distribution at the inflow boundary are summarized below.

Item	Description	Units	Default Value
WPEXP	exponent used to automatically generate the WPSCDL array	none	2.0*
NPSSUB	minimum number of particle streamlines starting from the submerged inflow boundary	none	2
WPSCDL	table of particle mass flow fractions for each streamline at the inflow boundary	none	10 * 0.0

*When WPEXP is set equal to 2.0, the code generates values of WPSCDL approximately equal to those used in the original FCT module.

Output Control

If particle impact occurs, the impact conditions are automatically printed out with the regular output (at the output steps specified by the NPRT vector in the TD2 namelist). The user can also ask for a printout detailing the particle streamline positions and crossover conditions at each output step by setting the logical variable PTPART to .TRUE.

The code also has provisions to print a detailed debug output which lists each iteration of the trajectory integration calculations. The debug output is obtained by setting the logical variable PTDTRJ to .TRUE. The reader is cautioned not to use the latter option indiscriminately since a massive output results.

A summary of the output control variables is given below.

Item		Description	Units	Default Value
PTPART	=	.TRUE., will result in a detailed printout of particle streamline positions and crossover conditions at each output step	logical	.FALSE.
PTDTRJ	=	.TRUE., will result in a debug printout of all trajectory integration iterations at each output step	logical	.FALSE.

Miscellaneous Variables

There are a number of other variables in the TD3 namelist used to facilitate calculations. Numerical instabilities in the gas flowfield are controlled by the variable DAMPN. If DAMPN is set to .TRUE., the gas pressure, density, and velocity components are smoothed using a fourth-order scheme described by Kutter (Reference 10). The smoothing is controlled by the coefficients SMLDI and SMLDJ in the x and y directions of the transformed

coordinate plane. The coefficients range in value from 0.0 (no smoothing) to 0.5 (maximum smoothing). Values between 0.05 and 0.3 are recommended.

Instabilities in the gas flowfield are especially critical during the early phase of the calculation. Stability is enhanced by allowing the gas flowfield to relax for a sufficient number of time steps before particle-gas coupling terms are introduced in the calculations. The variable NGIPI1 delays the particle trajectory calculations until NGIPI1 gas flowfield time steps have been executed. Values between 100 and 200 for NGIPI1 are recommended.

Savings in computational time can be effected by reducing the number of particle trajectory calculations. The number of gas phase calculation steps per set of particle phase calculations, defined by the variable NGIPI in the TD2 namelist, has been increased to 25 in CFC, thus decreasing the total number of particle trajectory calculations. These calculations can be further reduced by specifying only one particle size group. However, for impact calculations, trajectories of more than one size group are of interest. By setting the variable SPCUPL to .TRUE., the time-dependent calculations are performed with only one particle group, while the calculations at the final time step are performed with NPG particle groups. (The variable NPG is specified in the TD2 namelist.) The user can control the particle group used for the single-sized particle calculations through the variable KSPAR. It is recommended that KSPAR be set to the particle group corresponding to the mean particle size.

The variable WTROX is used to adjust the mass flux of aluminum particles impacting the wall. The code currently does not account for mass transfer beween the phases. Since it is important to obtain the correct choking conditions, and since the particle phase at the throat is comprised mostly of aluminum oxide, the variable WPWGT* should be based on the aluminum

oxide-to-gas mass ratio at the throat. However, since impact by aluminum agglomerate is of interest in the entrance region, the mass of particles impacting the wall must be adjusted by the Al/Al_2O_3 mass ratio. This ratio is specified in the TD3 namelist by the variable WTROX.

A summary of variables is given below.

Item		Description	Units	Default Value
DAMPN	=	.TRUE., will result in numerical smoothing of gas flowfield variables	logical	.FALSE.
SMLDI		smoothing coefficient in x direction of transformed coordinate plane	none	0.2
SMLDJ		smoothing coefficient in y direction of transformed coordinate plane	none	0.2
NGIPI1		number of gas phase calculation steps before first particle phase calculation	none	0
SPCUDL	=	.TRUE., will result in one particle size group being used in all calculations, except for the final step	none	.FALSE.
KSPAR		the particle size group to be used in above calculation $1 \leq$ USPAR $\leq$ NPG	none	1
WTROX		metal-to-metal oxide mass ratio WTROX = 0.5292 for aluminum	none	1.0

*WPWGT is the particle-to-gas weight flow ratio, and is input in the TD2 namelist.

SECTION 6

NEW OUTPUT FOR CFC

The output from the Chamber Flowfield Code is similar to the output from the FCT code except for some new tables and error messages. Most of the new output is self-explanatory. The major new tables and messages are described below.

Particle Impact Conditions

Impact conditions are printed automatically at each output step for each particle size group impinging upon the nozzle walls. An example of the printout is shown in Table 2. The variables in the table are described separately in Table 3. The conditions required to calculate erosion rates, such as particle velocity, angle of impact, and impingement mass flux, are printed in the output table along with the impact locations. The particle diameter is obtained from the particle group size.

Most of the values in the output table are nondimensional. To convert them to engineering units they must be multiplied by the normalizing quantities indicated in Table 3. The values of the normalizing quantities are printed near the beginning of the output.

Particle Streamline Details

Details of particle streamline relative positions, mass flow between adjacent streamlines, and other related variables can be printed out by the user, if desired. By setting PTPART to .True., two additional

Table 2. Example of Particle Impact Conditions Table Printout

PARTICLE IMPACT CONDITIONS

KK	L	I	X	Z	R	U	V	VTOT	THETAIMP	ROP	FLUXMP
1	5	1	.03410	-1.29093	1.95267						
2	5	2	.05000	-1.29325	1.91333	.02229	.00478	.02279	100.78392	.08209	.00187
3	4	2	.07128	-1.28702	1.86095						
4	4	3	.10000	-1.27865	1.79024	.03121	.00840	.03232	90.41181	.04860	.00157
5	4	4	.15000	-1.24163	1.67165	.03121	.00840	.03232	82.60879	.00176	.00006
6	4	5	.20000	-1.18536	1.56157	.03121	.00840	.03232	75.57077	.00011	.00000
7	3	5	.24587	-1.12089	1.46769						
8	3	6	.25000	-1.11508	1.45924	.03932	.00795	.04011	64.07091	.07339	.00294
9	3	7	.30000	-1.03012	1.36880	.03932	.00795	.04011	54.83381	.00474	.00019
10	3	8	.35000	-.93533	1.28886	.03932	.00795	.04011	48.30385	.00065	.00003
11	3	9	.40000	-.83272	1.21924	.03932	.00795	.04011	42.83365	.00016	.00001
12	3	10	.45000	-.72390	1.15997	.03932	.00795	.04011	38.14380	.00005	.00000
13	3	11	.50000	-.61030	1.11017	.03932	.00795	.04011	32.91927	.00002	.00000
14	3	12	.55000	-.49300	1.07000	.03932	.00795	.04011	28.49630	.00001	.00000
15	3	13	.60000	-.37188	1.03969	.03932	.00795	.04011	23.52494	.00001	.00000
16	3	14	.65000	-.24897	1.01778	.03932	.00795	.04011	19.68733	.00000	.00000
17	3	15	.70000	-.12482	1.00431	.03932	.00795	.04011	15.65875	.00000	.00000
18	3	16	.75000	.00000	1.00000	.03932	.00795	.04011	11.42730	.00000	.00000
19	3	17	.80000	.12481	1.00782	.03932	.00795	.04011	4.25495	.00000	.00000
20	3	18	.85000	.24768	1.03116	.03932	.00795	.04011	-2.91587	.00000	.00000

Table 3. Description of Variables in Particle Impact Conditions Table

Variable	Description	Units	Normalizing Quantity
KK	Sequence number	--	--
L	Particle streamline designation (old)*	--	--
I	Mesh point counter along transformed axial coordinate	--	--
X	Distance along the transformed axial coordinate	none	--
Z	Distance along the physical axial coordinate	none	Throat radius (RSI)
R	Distance along the physical radial coordinate	none	Throat radius (RSI)
U	Particle impact velocity component in the axial direction	none	AN
V	Particle impact velocity component in the radial direction	none	AN
VTOT	Magnitude of particle impact velocity vector	none	AN
THETA IMP	Particle impingement angle	degrees	--
ROP	Particle spatial density at impact location	none	RHON
FLUXMP	Particle impingement flux		AN X RHON

*New and old particle streamline numbers are described later in this section.

tables are printed for each particle size group at each output step. The first table gives the L(old)-L(new) matrix shown in Table 4. The L(old), L(new) particle streamline labeling scheme is explained in detail in Volume I of the Particle Impact Erosion Final Report (Reference 1). Essentially, the L(old) streamline label is applied sequentially to the streamlines at the inflow boundary, starting from 1 at the axis to NIPPG at the nozzle wall. The L(old) identifier remains fixed for each streamline. In comparison, the L(new) identifier depends upon the streamlines local position. At each constant X mesh location (i.e., at each value of I, the mesh counter in the X direction), the streamlines are renumbered starting from 1 at the axis and increasing with Y. The L(new) labels, therefore, define the relative positions of the streamlines at a given location, and these positions change with the occurrence of trajectory crossovers.

In cases where steamlines are terminated, the numbering scheme described above is slightly modified. Streamline terminations occur when subsequent streamlines impact the nozzle walls. In this case, the terminated streamlines are assigned to the top of the L(new) table and are removed from further calculations. Streamlines are also terminated if they return to the chamber wall, or if the trajectory calculations fail. In such cases, the streamlines are assigned to the bottom of the L(new) table from the outset, and are removed entirely from the particle density calculations. However, particle mass flux is conserved by redistribution among the remaining streamtubes.

An example of the second table printed, when PTPART is set to true, is shown in Table 5. The various quantities used in the particle spatial density are listed. The term VP.DA is the dot product of velocity and area between adjacent streamlines. DMDOTP is the mass flow rate between adjacent

Table 4. Example of L(old) - L(new) Matrix Printout

LOLD-LNEW MATRIX FOR KPB = 1

	I	L= 1	L= 2	L= 3	L= 4	L= 5	L= 6	L= 7	L= 8	L= 9	L= 10
OLD	1	1	2	3	4	5	6	7	8	9	10
NEW	1	1	2	3	4	5	6	7	8	9	10
OLD	2	1	2	3	4	6	7	8	9	10	5
NEW	2	1	2	3	4	10	5	6	7	8	9
OLD	3	1	2	3	6	7	8	9	10	4	5
NEW	3	1	2	3	9	10	4	5	6	7	8
OLD	4	1	2	3	6	7	8	9	10	4	5
NEW	4	1	2	3	9	10	4	5	6	7	8
OLD	5	1	2	3	6	7	8	9	10	4	5
NEW	5	1	2	3	9	10	4	5	6	7	8
OLD	6	1	2	6	7	8	9	10	3	4	5
NEW	6	1	2	8	9	10	3	4	5	6	7
OLD	7	1	2	6	7	8	9	10	3	4	5
NEW	7	1	2	8	9	10	3	4	5	6	7
OLD	8	1	2	6	7	8	9	10	3	4	5
NEW	8	1	2	8	9	10	3	4	5	6	7
OLD	9	1	6	2	7	8	9	10	3	4	5
NEW	9	1	3	8	9	10	2	4	5	6	7
OLD	10	1	7	6	2	8	9	10	3	4	5
NEW	10	1	4	8	9	10	3	2	5	6	7
OLD	11	1	7	8	6	9	10	2	3	4	5
NEW	11	1	7	8	9	10	4	2	3	5	6
OLD	12	1	7	8	9	10	6	2	3	4	5
NEW	12	1	7	8	9	10	6	2	3	4	5
OLD	13	1	7	8	9	10	6	2	3	4	5
NEW	13	1	7	8	9	10	6	2	3	4	5
OLD	14	1	8	7	10	9	6	2	3	4	5
NEW	14	1	7	8	9	10	6	3	2	5	4
OLD	15	1	8	7	10	9	6	2	3	4	5
NEW	15	1	7	8	9	10	6	3	2	5	4
OLD	16	1	8	7	10	9	6	2	3	4	5
NEW	16	1	7	8	9	10	6	3	2	5	4

Table 5. Example of ROP-YP and Other Arrays Printout

ROP-YP ARRAYS AND OTHER RELATED VARIABLES

I= 1	NPPAX= 10	IMPW= 0	ICR= 0									
VP.DA (LNEW)	.00000	.00000	.00000	.00000	.00000	.00000	.00000	.00000	.00000	.00000	.00000	.00000
DMDOTP(LNEW)	.00000	.01438	.01985	.02258	.02458	.02618	.02753	.02870	.02968	.02444		
ROP (LOLD)	.18016	.18029	.18082	.18130	.18131	.18123	.18102	.18240	.18452	.18358		
YP (LOLD)	.00000	.17465	.22613	.29298	.38272	.51641	.70198	.86667	.93088	.99700		
I= 2	NPPAX= 10	IMPW= 1	ICR= 1									
VP.DA (LNEW)	.00000	.07491	.11309	.08000	.24531	.13734	.19305	.08845	.09920	.00129	.00835	
DMDOTP(LNEW)	.00000	.01438	.01985	.02258	.00785	.03880	.04455	.03094	.03258	.00011		
ROP (LOLD)	.21766	.19203	.17553	.28226	.08209	.05200	.28253	.23078	.34982	.32841		
YP (LOLD)	.00000	.15974	.20529	.25596	1.00000	.47998	.67590	.85411	.92417	.99567		
I= 3	NPPAX= 9	IMPW= 1	ICR= 1									
VP.DA (LNEW)	.00000	.04989	.08699	.22807	.11889	.17614	.08648	.08518	.00093	.00831		
DMDOTP(LNEW)	.00000	.01438	.01985	.00732	.04458	.05311	.03515	.03672	.00003	.00000		
ROP (LOLD)	.37175	.28830	.22794	.04860	.00000	.03209	.37496	.30155	.40658	.43107		
YP (LOLD)	.00000	.14251	.18708	1.00000	1.00000	.43547	.63926	.84319	.91966	.99241		
I= 4	NPPAX= 9	IMPW= 1	ICR= 0									
VP.DA (LNEW)	.00000	.03026	.05706	.16404	.10175	.16305	.08151	.07297	.00087	.01589		
DMDOTP(LNEW)	.00000	.01438	.01985	.00732	.04458	.05311	.03515	.03672	.00000	.00000		
ROP (LOLD)	.62661	.47539	.34747	.00176	.00000	.04462	.43813	.32573	.43120	.50321		
YP (LOLD)	.00000	.12225	.16609	1.00000	1.00000	.38050	.59610	.82840	.91243	.98679		
I= 5	NPPAX= 9	IMPW= 1	ICR= 0									
VP.DA (LNEW)	.00000	.01583	.03345	.11112	.08587	.14940	.07702	.06201	.00136	.01264		
DMDOTP(LNEW)	.00000	.01438	.01985	.00732	.04458	.05311	.03515	.03672	.00000	.00000		
ROP (LOLD)	1.20124	.90853	.59276	.00011	.00000	.06587	.51918	.35549	.45653	.59214		
YP (LOLD)	.00000	.09783	.14105	1.00000	1.00000	.31123	.54210	.80882	.90240	.97842		
I= 6	NPPAX= 8	IMPW= 1	ICR= 1									
VP.DA (LNEW)	.00000	.00616	.05513	.06992	.13475	.07290	.05178	.00090	.00111			
DMDOTP(LNEW)	.00000	.01438	.00283	.04971	.06300	.04050	.04052	.00007	.00000	.00000		
ROP (LOLD)	2.56021	2.33346	.07359	.00000	.00000	.05130	.71097	.46753	.55551	.78250		
YP (LOLD)	.00000	.06784	1.00000	1.00000	1.00000	.22565	.47360	.78259	.88879	.96608		
I= 7	NPPAX= 8	IMPW= 1	ICR= 0									
VP.DA (LNEW)	.00000	.00097	.01613	.04555	.11878	.06927	.04182	.00197	.01197			
DMDOTP(LNEW)	.00000	.01438	.00283	.04971	.06300	.04050	.04052	.00001	.00000	.00000		
ROP (LOLD)	15.64858	14.83728	.00474	.00000	.00000	.17534	1.09154	.53038	.58459	.96883		
YP (LOLD)	.00000	.03011	1.00000	1.00000	1.00000	.13149	.38494	.74629	.87029	.94728		

streamlines, and ROP represents the particle spatial density in that region. The last term, YP, is the location of the particle streamline in the transformed Y coordinate.

The table also indicates the presence of wall impact or trajectory crossover, at each value of I, by the variables IMPW and ICR. The maximum and minimum values of streamlines are also printed, indicating the number of streamlines terminated. The number of entries for VP.DA generally exceeds the maximum number of streamlines. The extra location is used to store wall impact conditions.

Trajectory Integration Details

Details of each iteration of the particle trajectory calculations can be printed out by the user by setting PTDIRJ to .True. An example of the output is partially reproduced in Table 6. The output shown is for the first particle group (K = 1) and the first streamline (L = 1). The iteration number is given in the first column. The rest of the variables have their usual meanings. Variables followed by 1 refer to the starting values of those variables for each set of iterations. Variables followed by 2 refer to their values after each iteration.

Since the total printout of this table is massive, it should be used mainly for debugging purposes. It can also be used to check the details of particle trajectories, since the regular printout lists streamline positions only at each constant X mesh location. If the particle crosses the same mesh line twice, the particle conditions at those locations are written over and some portions of the trajectory may go unrecorded. This is especially true for particles which cross the axis, and is the reason why particle streamline plots sometimes look jagged and discontinuous. It should be emphasized that although intermediate particle locations and conditions may not be stored and

Table 6. Example of Particle Integration Calculations Table

IT	I	I1	I2	J1	J2	X1	X2	Y1	Y2	UP1	UP2	VP1	VP2	TP2
K= 1		L= 1												
1	1	1	2	1	1	.0000	.5000-01	.0000	.0000	.1000-04	.3262-02	.0000	.0000	.1083+01
2	1	1	2	1	1	.0000	.5000-01	.0000	.0000	.1000-04	.3026-02	.0000	.0000	.1083+01
3	1	1	2	1	1	.0000	.5000-01	.0000	.0000	.1000-04	.3051-02	.0000	.0000	.1083+01
4	1	1	2	1	1	.0000	.5000-01	.0000	.0000	.1000-04	.3049-02	.0000	.0000	.1083+01
5	1	1	2	1	1	.0000	.5000-01	.0000	.0000	.1000-04	.3049-02	.0000	.0000	.1083+01
1	2	2	3	1	1	.5000-01	.1000+00	.0000	.0000	.3049-02	.4445-02	.0000	.0000	.1083+01
2	2	2	3	1	1	.5000-01	.1000+00	.0000	.0000	.3049-02	.4391-02	.0000	.0000	.1083+01
3	2	2	3	1	1	.5000-01	.1000+00	.0000	.0000	.3049-02	.4395-02	.0000	.0000	.1083+01
4	2	2	3	1	1	.5000-01	.1000+00	.0000	.0000	.3049-02	.4395-02	.0000	.0000	.1083+01
1	3	3	4	1	1	.1000+00	.1500+00	.0000	.0000	.4375-02	.5662-02	.0000	.0000	.1083+01
2	3	3	4	1	1	.1000+00	.1500+00	.0000	.0000	.4375-02	.5645-02	.0000	.0000	.1083+01
3	3	3	4	1	1	.1000+00	.1500+00	.0000	.0000	.4395-02	.5646-02	.0000	.0000	.1083+01
4	3	3	4	1	1	.1000+00	.1500+00	.0000	.0000	.4375-02	.5646-02	.0000	.0000	.1083+01
1	4	4	5	1	1	.1500+00	.2000+00	.0000	.0000	.5646-02	.7010-02	.0000	.0000	.1083+01
2	4	4	5	1	1	.1500+00	.2000+00	.0000	.0000	.5646-02	.7013-02	.0000	.0000	.1083+01
3	4	4	5	1	1	.1500+00	.2000+00	.0000	.0000	.5646-02	.7013-02	.0000	.0000	.1083+01
1	5	5	6	1	1	.2000+00	.2500+00	.0000	.0000	.7013-02	.8634-02	.0000	.0000	.1083+01
2	5	5	6	1	1	.2000+00	.2500+00	.0000	.0000	.7013-02	.8653-02	.0000	.0000	.1083+01
3	5	5	6	1	1	.2000+00	.2500+00	.0000	.0000	.7013-02	.8652-02	.0000	.0000	.1083+01
4	5	5	6	1	1	.2000+00	.2500+00	.0000	.0000	.7013-02	.8652-02	.0000	.0000	.1083+01
1	6	6	7	1	1	.2500+00	.3000+00	.0000	.0000	.8652-02	.1071-01	.0000	.0000	.1083+01
2	6	6	7	1	1	.2500+00	.3000+00	.0000	.0000	.8652-02	.1075-01	.0000	.0000	.1083+01
3	6	6	7	1	1	.2500+00	.3000+00	.0000	.0000	.8652-02	.1075-01	.0000	.0000	.1083+01
4	6	6	7	1	1	.2500+00	.3000+00	.0000	.0000	.8652-02	.1075-01	.0000	.0000	.1083+01
1	7	7	8	1	1	.3000+00	.3500+00	.0000	.0000	.1075-01	.1353-01	.0000	.0000	.1083+01
2	7	7	8	1	1	.3000+00	.3500+00	.0000	.0000	.1075-01	.1358-01	.0000	.0000	.1083+01
3	7	7	8	1	1	.3000+00	.3500+00	.0000	.0000	.1075-01	.1358-01	.0000	.0000	.1083+01
4	7	7	8	1	1	.3000+00	.3500+00	.0000	.0000	.1075-01	.1358-01	.0000	.0000	.1083+01
1	8	8	9	1	1	.3500+00	.4000+00	.0000	.0000	.1358-01	.1758-01	.0000	.0000	.1083+01
2	8	8	9	1	1	.3500+00	.4000+00	.0000	.0000	.1358-01	.1767-01	.0000	.0000	.1083+01
3	8	8	9	1	1	.3500+00	.4000+00	.0000	.0000	.1358-01	.1767-01	.0000	.0000	.1083+01
4	8	8	9	1	1	.3500+00	.4000+00	.0000	.0000	.1358-01	.1767-01	.0000	.0000	.1083+01
1	9	9	10	1	1	.4000+00	.4500+00	.0000	.0000	.1767-01	.2408-01	.0000	.0000	.1083+01
2	9	9	10	1	1	.4000+00	.4500+00	.0000	.0000	.1767-01	.2445-01	.0000	.0000	.1083+01
3	9	9	10	1	1	.4000+00	.4500+00	.0000	.0000	.1767-01	.2442-01	.0000	.0000	.1083+01
4	9	9	10	1	1	.4000+00	.4500+00	.0000	.0000	.1767-01	.2442-01	.0000	.0000	.1083+01
5	9	9	10	1	1	.4000+00	.4500+00	.0000	.0000	.1767-01	.2442-01	.0000	.0000	.1083+01
1	10	10	11	1	1	.4500+00	.5000+00	.0000	.0000	.2442-01	.3922-01	.0000	.0000	.1083+01
2	10	10	11	1	1	.4500+00	.5000+00	.0000	.0000	.2442-01	.3972-01	.0000	.0000	.1083+01
3	10	10	11	1	1	.4500+00	.5000+00	.0000	.0000	.2442-01	.3967-01	.0000	.0000	.1083+01
4	10	10	11	1	1	.4500+00	.5000+00	.0000	.0000	.2442-01	.3967-01	.0000	.0000	.1083+01
5	10	10	11	1	1	.4500+00	.5000+00	.0000	.0000	.2442-01	.3967-01	.0000	.0000	.1083+01
1	11	11	12	1	1	.5000+00	.5500+00	.0000	.0000	.3967-01	.7711-01	.0000	.0000	.1081+01
2	11	11	12	1	1	.5000+00	.5500+00	.0000	.0000	.3967-01	.7792-01	.0000	.0000	.1081+01
3	11	11	12	1	1	.5000+00	.5500+00	.0000	.0000	.3967-01	.7782-01	.0000	.0000	.1081+01
4	11	11	12	1	1	.5000+00	.5500+00	.0000	.0000	.3967-01	.7783-01	.0000	.0000	.1081+01
5	11	11	12	1	1	.5000+00	.5500+00	.0000	.0000	.3967-01	.7783-01	.0000	.0000	.1081+01

plotted, the particle trajectories are calculated correctly, as may be verified by printing the detailed trajectory table.

Miscellaneous New Tables

The code prints the WPSCDL and DMDOTP arrays at the initial line for each particle group at each output step. An example is shown in Table 7. The variable WPSCDL was described earlier. If the option to calculate WPSCDL internally by specifying WPEXP is employed, the calculated values of WPSCDL will appear here. Since the calculated values may vary slightly at each iteration step, they are not printed toward the front of the output as are the input values of WPSCDL. The DMDOTP array at the initial line is different from the array described earlier. Here the variable refers to the particle mass flow rate between adjacent mesh points at the chamber boundary.

The code also prints a table toward the front of the output which lists the inflow boundary conditions at each mesh point along the chamber boundary. An example is given in Table 8. These may differ from the input values, since the mesh point values are obtained by interpolation along the boundary length. The table may be used to check the input and interpolated values of the boundary conditions.

Error Messages

The code prints error messages if it encounters problems during execution. Errors occur most commonly during particle trajectory calculations, examples of which are shown in Table 9. In CFC, the effect of errors is generally not as catastrophic as in FCT. Logic was introduced in the code to minimize the problems and inaccuracies associated with the errors, and to continue with the main body of calculations. The first error message in Table 9 serves as an example of this procedure. It indicates a failure to converge in the particle trajectory integration calculations. In order to

Table 7. Example of WPSCDL and DMDOT Arrays at the Inflow Boundary

WPSCDL AND DMDOT ARRAYS AT INITIAL LINE

WPSCDL	.00000	.01940	.07762	.17464	.31047	.48511	.69856	.78564	.88612	1.00000
DMDOTP	.00000	.00155	.00452	.00690	.00734	.00570	.00396	.00389	.00389	.00389
	.00388	.00387	.00384	.00642	.00897	.00758				

Table 8. Example of Table of Boundary Conditions at Mesh Points

J	CHAMBER WALL ANGLE	INITIAL GAS FLOW ANGLE	INITIAL PARTICLE FLOW ANGLE	GRAIN/FLOW AREA PERIMETER RATIO	BURN LAW CONSTANT	BURN LAW EXPONENT
1	89.9942732	-.0057263	-.0057263	2.3895000	1.7430000	.3097700
2	88.9048138	-1.0951850	-1.0951850	2.3895000	1.7430000	.3097700
3	70.0500011	-19.9499979	-19.9499979	2.3895000	1.7430000	.3097700
4	33.4414954	-56.5585041	-56.5585041	2.3895000	1.7430000	.3097700
5	7.1058088	-82.8941908	-82.8941908	1.8975990	1.7430000	.3097700
6	-.1890349	89.8109646	89.8109646	1.0349731	1.7430000	.3097700
7	.0355867	-89.9644127	-89.9644127	1.0000000	1.7430000	.3097700
8	.0355867	-89.9644127	-89.9644127	1.0000000	1.7430000	.3097700
9	.0355876	-89.9644117	-89.9644117	1.0000000	1.7430000	.3097700
10	.0354997	-89.9645004	-89.9645004	1.0000000	1.7430000	.3097700
11	.0333470	-89.9666529	-89.9666529	1.0000000	1.7430000	.3097700
12	.0555944	-89.9444046	-89.9444046	1.0000000	1.7430000	.3097700
13	-9.0144306	80.9855690	80.9855690	1.0000000	1.7430000	.3097700
14	-22.5267856	67.4732141	67.4732141	3.3544000	1.7430000	.3097700
15	-24.5399590	65.4600401	65.4600401	3.3544000	1.7430000	.3097700
16	-8.7599970	81.2400017	81.2400017	3.3544000	1.7430000	.3097700

Table 9. Examples of Particle Trajectory Calculations Error Messages

1.
```
PARTICLE INTEGRATION FAILED TO CONVERGE AT STATION 11 ,INTEGRATION NUMBER  7 ,PARTICLE GROUP  1
AFTER 31 ITERATIONS ON STEP NO. 650
 UP,VP,TP,UPO AND VPO ARE      .1192101      -.0338729      1.0880056      .0723908      -.0252734
 I1,I2,J1,J2,FACE AND FO ARE   11   12   10   10   1   1
```

2.
```
XYLOC ERROR AT NSTEP= 650      K=  1     L=  3     I= 11
     I1,I2,J1,J2,X1,X2,Y1,Y2 ARE   11   11    8    8    .5111165    .5111165    .5333333    .5333333
```

3.
```
PARTICLE RETURNS TO CHAMBER AT   NSTEP= 650      K=  3     L=  3     I=  5
     I1,I2,J1,J2,X1,X2,Y1,Y2 ARE    1    0   11   11    .0293510    .0000000    .6666667    .7151821
```

4.
```
TOO MANY IMPACTS PER STEP
PARTICLE GROUP =    2     NSTEP =  800
I =    4     KK =    2     LPW(KK) =    7     LPW(KK-1) =    5     XPW(KK) =    .091301     XPW(KK-1) =    .088394
```

increase the chances of convergence, the number of iterations have been increased to 30 in CFC. Also, it was found that even in cases where the integration had not formally converged in 30 iterations, the values were very close to the final solution. Hence, the particle trajectory calculations in CFC continue forward from the last iteration step even if the integration has not fully converged. A message, however, is printed to inform the user of this occurence.

The second error message in Table 9 is printed when a streamline encounters problems in the XYLOC subroutine, which calculates the position of the streamlines on the X-Y mesh. If the local mesh geometry is poor, the streamline may become trapped within a mesh cell. In this case, the entire streamline is terminated by the code (cf., earlier discussion). The particle mass flow associated with the streamline is distributed among adjacent streamlines, so that the total particle mass flow is conserved. Hence, the code calculations are unaffected by the error except for a degradation in the particle flowfield resolution.

The third error message in Table 9 occurs when a streamline returns to the inflow boundary. Presently the code cannot handle these situations, and the streamlines are terminated as with XYLOC errors.

The final error message occurs when two or more streamlines impact the nozzle wall between two adjacent mesh points, a situation the code logic cannot currently handle. If this error occurs during the final time step of a run, it may result in problems since the impact conditions will not be known. The user may attempt to eliminate the error by rerunning the case with different values of WPSCDL for the impacting streamlines.

SECTION 7

SAMPLE PROBLEM USING CFC

The Hercules NTF 001 nozzle, fired on a Brutus motor, was used to demonstrate the subsonic-transonic total recession prediction methodology developed for the Particle Impact Erosion Program. Details of the firing, the actual chamber and nozzle geometries, and the approximations made for the CFC calculations are given in Reference 1. The CFC results at an early burn time are presented here as a sample problem.

The input data list for the sample problem is shown in Table 10. The properties previously communicated to FCT from ODE were obtained from ACE (Reference 9) calculations. A summary of the ACE results is shown in Table 11. Average properties between the chamber and throat were used in CFC. Also, since the expansion in CFC extends only to the transonic region, the expansion ratio (EPM), gas velocity (UGM), and particle temperature (TPM) were selected at a location where the Mach number was slightly greater than one, rather than where the particle melt temperature occurs. (See column labeled location "M" in Table 11). The particle latent heat (DHM) was, therefore, dummied by selecting a very small (negligible) value. The TPS and UGS values were selected at a higher Mach number (Column labeled location "S" in Table 11).

Selected outputs are shown in Table 12. The particle impact conditions and other parameters are shown at the 1,000th time step. The

Table 10. CFC Sample Problem Input

```
TITLE TEST CASE 14 -- NTF-001   ZERO BURN TIME   GEOM #5B
SPP
 $SPP
  TD2P=1.,
  RSI = 2.250,
  INLET = 3, PHI = 88.0, RWTU=1.350,
  ZI = -1.5111,  RI =  2.0533,
  IWALL=3, RWTD=1.350, THETA=14.40, EPS=3.0,
  CMNT = 0.1, 0.3, 0.5, 0.7, 0.9, 1.0, 1.1, NCMNT = 7,
  CPRT = 1.6, 1.5, 1.4, 1.3, 1.1, 1.0, 0.8, 0.6, 0.4, NCPRT=9,
   PLTT=1, PRNTPL=1, NPLTS=2*1,0,3*1, NSPLTS=2*1,0,3*1,
 $END
 $TD2
  PR = 0.41125, GMGO = 0.46646E-04, CAPN = 0.6607,
  CPS = 8498.0, CPL = 8498.0,
  TPM = 4759.1, DHM = 1.0E-06, EPM = 1.1600, UGM = 4325.,
  TPS = 4573.9, UGS = 4808.,
  PC = 835.0, TGO = 5497.8,
  WPWGT = 0.50693,
  REG2 = .TRUE., PTRAJP = .TRUE., ZMAXA=2.00,
  NX = 31, NY = 21,
  PKK = 105*0.2,  PLK = 105*0.5,
   ITHIN=1, POIN=21*1.0, TOIN=21*1.0,
   THIN = 1.0E-06,19*-89.0,-92.0,
   IPCALC=1,
   THPK(1,1)= 0.0,19*-89.0,-92.0,
   THPK(1,2)= 0.0,19*-89.0,-92.0,
   THPK(1,3)= 0.0,19*-89.0,-92.0,
   NPRT=3*1000, NPLT=3*1000,
 $END
 $TD3
  RDOT = 0.3557,
  ALFAAP = 0.70,
  IPATCH = 3,
  ZPATCH =  -8.0000,-4.4056,-0.81127,
  RPATCH =   0.000,  0.5997, 1.19931,
  ICHMB=11, ICHMB2=8, ICHMB1=4,
  ZCHMB = -47.619,-47.618,-47.617,-47.616,
          -43.172,-38.728,-34.284,-29.840,
                  -19.170,-10.340, -1.5117,
  RCHMB =   0.000,  1.038,  2.076,  3.114,
            3.113,  3.112,  3.111,  3.110,
                    2.765,  2.420,  2.0743,
  FPERCH = 11*1.0,
  BEXPCH = 11*0.343,   CBRNCH = 11*0.3874,
   SPCUPL=.TRUE., KSPAR=2,
  PTPART = .TRUE., NGIPII = 200, WIROX = 0.5292,
  WPEXP = 1.0, NPSSUR = 5,
  DAMPN = .TRUE., SMLDI = 0.3, SMLDJ = 0.3,
 $END
```

Table 11. ACE Run Results Used in Sample Problem

Location	Chamber	Throat	M	S
Pressure (atm)	60.45[a]	34.615	20.0	15.0
Mach number		1.0	1.433	1.624
Temperature (°R)	5,497.8[b]	5,120.4	4,759.1	4,573.9
Particle enthalpy $\left(\frac{\text{Btu}}{\text{lbm°R}}\right)$	-5,045.6	-5,173.8		
Particle to gas mass ratio	0.49916	0.50693		
Gas viscosity $\left(\frac{\text{lbm}}{\text{ft/sec}}\right)$	0.4665×10^{-4}	0.4450×10^{-4}		
Gas Prandtl number	0.41042	0.41209		
Velocity $\left(\frac{\text{ft}}{\text{sec}}\right)$		3,127	4,325	4,808
Expansion ratio		1.000	1.160	

[a]Average chamber pressure = 888.6 psia
[b]Flame temperature (heat loss to exposed insulation in aft closure considered)

Table 12. CFC Sample Problem Output

```
                TWO DIMENSIONAL - TWO PHASE FLOW LOSS MODEL (TDPP)

                      TEST CASE 14 -- NTF-001   ZERO BURN TIME   GEOM #58

                       INPUT CONDITIONS
          PC=          835.000          TG=          5497.800
          LSTAR=         0.000          NPG=                5
          GMGJ=       .4665E-04         CAPN=          .66070
          WPWGT=         .50693         WT FRAC=       .33640
          RRT=          1.35000         RWID=         1.35000
          THID=        12.99794          THJW=        14.40000
          IWALL=              5         PGFIG=         0.00000
          CPL=          8498.0          XMLW=         26.98154
          UGS=          4809.000        TPS=          4573.900
          VEMPTY=          0.0          WPROP=           0.0
          RHPROP=       0.00000         SMP=          147.600
          ALFA=           .3000         DL=            .10000
          DR=             .10000        DTWI=         3.50000
          DHIT=           .01000        EW=            .30100
          IMAX=                5        N1=              1000
          N2=                  1        NTBL=              15
          XITBL=         0.0000

G(I)=     .1151165E+01 E(I)=     .1160000E+01
CPG =     .1477162E+05   G GAS=.1204254E+01 RCAP =   .2505421E+04
CPS =     .8498000E+04 HPS =     .4044283E+08 HPL =     .4044283E+08 HPO =    .4672030E+08  PR =   .4112500E+00
RHOGO=    .2808564E+00   R =     .1166686E+01  RS =     .1166686E+01 GSR =    .1151165E+01
          UGM=         4325.000          TPM=          4759.100
          EPM=           1.1600          OHM=       1.0000E-06

           MEAN PARTICLE DIAMETER(MICRONS)=  140.57
                PARTICLE SIZE DISTRIBUTION

     GROUP    R(FT)          D(MICRONS)          WPWT
       1    .1478E-03          90.122           .33333
       2    .2307E-03         140.66            .33333
       3    .3602E-03         219.56            .33333
```

Table 12. (Continued)

```
FCT TRANSONIC MODULE

 NORMALIZING          ENGR              INTERNAL          SI
  QUANTITY            UNITS             UNITS             UNITS

     PN=                566.777 PSI       81615.95 PSF      3907.8 KPA
     AN=               1879.521 FT/S      1879.521 FT/S    1182.4779 M/S
     TN=               4988.354 DEG R     4988.354 DEG R   2771.3078 DEG K
     RHON=                .1795 LBM/FT3     .005923 SL/FT3     2.795 KG/M3
     RGASN=             93.78 FT-LBF/LBM  3017.16 (FT/S)**2    .5096 KJ/KG K

                    MESH CONTROL DATA

NX=   31          NY=   21
ZMAXA=     2.00000 ZMAXW=      .13573  RMAXW=     1.04201  ZMINW1=     -.81127 RMINW1=     1.19931
ZMINA1=  -8.00000  ZMINW2=   -1.51070  RMINW2=     2.07430 ZMINA2=   -47.61903
IGR1=    2         IGR2=    1         REG2=    T

                    TIME STEP CONTROL

CNO=     1.00000   NSMAX= 1000

                    PARTICLE INTEGRATION CONTROL

NPG=    3          NIPPG=   10          NGIPI=   25

NPSCOL =  0.00000   0.00000   0.00000   0.00000   0.00000   0.00000   0.00000   0.00000   0.00000   0.00000

                    PRINT - PLOT FREQUENCY CONTROL

     NPRT=   1000   1000   1000      NPLT=   1000   1000   1000     NOPRT= 0
.18000006E+03     .88000029E+02     .25894623E+02
.18018006E+03     .88000029E+02     .25525356E+02
.17657589E+03     .88000029E+02     .24784252E+02
.17304380E+03     .88000029E+02     .23660519E+02
.16958235E+03     .88000029E+02     .21739807E+02
.16619013E+03     .88000029E+02     .17674015E+02
.16286575E+03     .88000029E+02     .31556041E+01
.16214319E+03     .88000029E+02    -.77575911E+01
.16264253E+03     .88000029E+02     .64281367E+00
.16259845E+03     .88000029E+02     .13734124E+00
.16237082E+03     .88000029E+02    -.30578562E+01
.16258867E+03     .88000029E+02     .11275673E-01
.16258773E+03     .88000029E+02     .13782627E-02
.16247928E+03     .88000029E+02    -.19503944E+01
.16254765E+03     .88000029E+02     .61484816E-04
.16258765E+03     .88000029E+02     .29573671E-05
  2.8377
 -.59303E-02
  2.8377        -.33593          2.2247          2.3744          -1.0313          -1.5107          .50242
  2.8338        -.33745          2.2247          2.3733          -1.0313          -1.5109          .50311
  2.8298        -.33176          2.2247          2.3722          -1.0313          -1.5109          .50381
  2.8259        -.31969          2.2247          2.3681          -1.0313          -1.5109          .50451
  2.8220        -.31963          2.2247          2.3660          -1.0313          -1.5110          .50522
  2.8180        -.32356          2.2247          2.3639          -1.0313          -1.5110          .50592
  2.8141        -.32749          2.2247          2.3611          -1.0313          -1.5110          .50663
  2.8102        -.33142          2.2247          2.3597          -1.0313          -1.5111          .50734
  2.8062        -.33535          2.2247          2.3576          -1.0313          -1.5111          .50805
```

Table 12. (Continued)

PARTICLE IMPACT CONDITIONS

PARTICLE GROUP = 2

KK	L	I	X	Z	R	U	V	VTOT	THETAIMP	ROP	FLUXMP
1	9	6	.19137	-1.40734	1.69252						
2	9	7	.20000	-1.39857	1.67671	.05958	-.00719	.06001	51.85777	.31751	.01808
3	9	8	.23333	-1.35996	1.61852	.05958	-.00719	.06001	47.46155	.38362	.01218
4	9	9	.26667	-1.31717	1.56535	.05958	-.00719	.06001	43.36133	.48067	.01526
5	9	10	.30000	-1.27067	1.51123	.05958	-.00719	.06001	39.54578	.56623	.01798
6	9	11	.33333	-1.22093	1.46222	.05958	-.00719	.06001	35.99864	.71457	.02269
7	9	12	.36667	-1.16834	1.41627	.05958	-.00719	.06001	32.70084	.97665	.03102
8	7	12	.39867	-1.11515	1.37076						
9	7	13	.40000	-1.11329	1.37331	.14536	-.01868	.14655	29.19526	.22092	.01713
10	7	14	.43333	-1.05610	1.33323	.14536	-.01868	.14655	26.33203	.22537	.01753
11	7	15	.46667	-.99706	1.29591	.14536	-.01868	.14655	23.68053	.22868	.01779
12	7	16	.50000	-.93643	1.26125	.14536	-.01868	.14655	21.28539	.23163	.01796
13	7	17	.53333	-.87445	1.22911	.14536	-.01868	.14655	19.03642	.23427	.01817
14	7	18	.56667	-.81127	1.19931	.14536	-.01868	.14655	16.90499	.25847	.02008
15	7	19	.60000	-.67965	1.14534	.14536	-.01868	.14655	13.20432	.25211	.01955
16	7	20	.63333	-.55514	1.10259	.14536	-.01868	.14655	10.26437	.22663	.01758
17	6	20	.65863	-.49493	1.08488						
18	6	21	.66667	-.43918	1.06850	.20739	-.03792	.21083	9.87882	.07796	.00870
19	6	22	.70000	-.33295	1.04177	.20739	-.03792	.21083	3.87362	.07962	.00888
20	6	23	.73333	-.23430	1.02049	.20739	-.03792	.21083	-.36715	.07974	.00890

PARTICLE DENSITIES AND COUPLING TERMS FOR PARTICLE GROUP NUMBER 2 TIME= 16.733458 NSTEP= 1888

I= 1 K= 0.0000 ZW= -1.51873 RW= 2.074395 RDOT P= .156985

J	RHO-P	UP	VP	TP	AP	BP	FPU	FPV	BP
1	1.30881E+00	1.00000E-05	0.	5.51064E-01	1.27511E-03	1.00913E-02	-1.66626E-08	0.	-6.97927E-03
2	1.30881E+00	9.76577E-06	-5.81934E-05	5.51064E-01	1.55153E-03	1.21398E-02	1.01260E-06	1.07270E-03	-6.09899E-03
3	1.30881E+00	9.55154E-06	-1.16387E-04	5.51064E-01	1.74999E-03	1.41884E-02	8.08894E-08	-5.64073E-06	-1.82332E-02
4	1.30881E+00	9.29731E-06	-1.74580E-04	5.51064E-01	2.04836E-03	1.62378E-02	8.38662E-08	-5.76468E-06	-1.17187E-02
5	1.30881E+00	9.06309E-06	-2.32773E-04	5.51064E-01	2.33677E-03	1.82856E-02	9.76816E-08	-6.45648E-06	-1.31882E-02
6	1.30881E+00	8.82886E-06	-2.90967E-04	5.51064E-01	2.56518E-03	2.03342E-02	1.09609E-07	-7.08878E-06	-1.46657E-02
7	1.30881E+00	8.59463E-06	-3.49160E-04	5.51064E-01	2.82563E-03	2.23828E-02	1.20483E-07	-7.43173E-06	-1.61432E-02
8	1.30881E+00	8.36040E-06	-4.07354E-04	5.51064E-01	3.08201E-03	2.44314E-02	1.31039E-07	-7.79605E-06	-1.76207E-02
9	1.29880E+00	8.12617E-06	-4.65547E-04	5.51064E-01	3.34043E-03	2.64800E-02	1.41023E-07	-8.07916E-06	-1.89522E-02
10	1.29880E+00	8.14969E-06	-4.66894E-04	5.51064E-01	3.33922E-03	2.64703E-02	1.40929E-07	-8.07379E-06	-1.89452E-02
11	1.29880E+00	8.17321E-06	-4.68241E-04	5.51064E-01	3.33801E-03	2.64606E-02	1.41705E-07	-8.11026E-06	-1.89383E-02
12	1.25330E+00	8.26204E-06	-4.73331E-04	5.51064E-01	3.31073E-03	2.64023E-02	1.37685E-07	-7.88796E-06	-1.82347E-02
13	1.25330E+00	8.35267E-06	-4.78523E-04	5.51064E-01	3.28329E-03	2.63429E-02	1.39083E-07	-7.96806E-06	-1.81936E-02
14	1.18342E+00	8.42269E-06	-4.82534E-04	5.51064E-01	3.31764E-03	2.62976E-02	1.32995E-07	-7.61923E-06	-1.71496E-02
15	1.18342E+00	8.48810E-06	-4.86282E-04	5.51064E-01	3.31219E-03	2.62556E-02	1.34681E-07	-7.71586E-06	-1.71222E-02
16	1.18342E+00	8.55352E-06	-4.90029E-04	5.51064E-01	3.30715E-03	2.62137E-02	1.36114E-07	-7.79795E-06	-1.70949E-02
17	1.18342E+00	8.61893E-06	-4.93777E-04	5.51064E-01	3.30190E-03	2.61717E-02	1.36844E-07	-7.83980E-06	-1.70675E-02
18	1.18342E+00	8.68434E-06	-4.97524E-04	5.51064E-01	3.29666E-03	2.61297E-02	1.35942E-07	-7.78887E-06	-1.70402E-02

I= 2 K= .0333 ZW= -1.5091A RW= 2.004607 RDOT P= .139161

J	RHO-P	UP	VP	TP	AP	BP	FPU	FPV	BP
1	0.14696E+00	1.00000E-05	0.	1.07754E+00	1.38570E-02	1.09676E-01	-3.33080E-03	0.	1.66956E-04
2	0.14696E+00	-1.36775E-04	-1.29269E-04	1.05119E+00	1.24040E-02	9.83494E-02	-2.72725E-03	3.81027E-03	-1.03343E-02
3	0.14696E+00	-2.83559E-04	-2.58538E-04	1.02483E+00	1.09790E-02	8.70232E-02	-1.24951E-03	3.99449E-04	-2.27805E-02
4	0.14696E+00	-4.30329E-04	-3.87807E-04	9.98672E-01	9.54998E-03	7.56977E-02	-3.31378E-04	-6.76232E-04	-2.86898E-02
5	0.14696E+00	-5.77100E-04	-5.17076E-04	9.72115E-01	8.17100E-03	6.43703E-02	-3.46224E-05	-3.27691E-04	-3.09957E-02
6	0.14696E+00	-7.23870E-04	-6.46345E-04	9.45757E-01	6.69201E-03	5.30446E-02	-1.19349E-05	-8.63364E-05	-3.15586E-02
7	0.14696E+00	-8.70650E-04	-7.75614E-04	9.19400E-01	5.26302E-03	4.17186E-02	-4.69166E-05	-2.65389E-05	-2.98689E-02

Table 12. (Continued)

OLD-NEW MATRIX FOR KPG = 2

	1	L= 1	2	3	4	5	6	7	8	9	10
OLD	1	2	3	4	8	10	1	5	6	7	9
NEW	1	6	1	2	3	7	8	9	4	10	5
OLD	2	2	3	4	8	10	1	5	6	7	9
NEW	2	6	1	2	3	7	8	9	4	10	5
OLD	3	2	3	4	8	10	1	5	6	7	9
NEW	3	6	1	2	3	7	8	9	4	10	5
OLD	4	2	3	4	8	10	1	5	6	7	9
NEW	4	6	1	2	3	7	8	9	4	10	5
OLD	5	2	3	4	8	10	1	5	6	7	9
NEW	5	6	1	2	3	7	8	9	4	10	5
OLD	6	2	3	4	8	10	1	5	6	7	9
NEW	6	6	1	2	3	7	8	9	4	10	5
OLD	7	2	3	4	8	10	1	5	6	7	9
NEW	7	6	1	2	3	7	8	9	4	10	5
OLD	8	2	3	4	8	10	1	5	6	7	9
NEW	8	6	1	2	3	7	8	9	4	10	5
OLD	9	2	3	4	8	10	1	5	6	7	9
NEW	9	6	1	2	3	7	8	9	4	10	5
OLD	10	2	3	4	8	10	1	5	6	7	9
NEW	10	6	1	2	3	7	8	9	4	10	5
OLD	11	2	3	4	8	10	1	5	6	7	9
NEW	11	6	1	2	3	7	8	9	4	10	5
OLD	12	2	3	4	8	10	1	5	6	7	9
NEW	12	6	1	2	3	7	8	9	4	10	5
OLD	13	2	3	4	8	10	1	5	6	7	9
NEW	13	6	1	2	3	7	8	9	4	10	5
OLD	14	2	3	4	8	10	1	5	6	7	9
NEW	14	6	1	2	3	7	8	9	4	10	5
OLD	15	2	3	4	8	10	1	5	6	7	9
NEW	15	6	1	2	3	7	8	9	4	10	5
OLD	16	2	3	4	8	10	1	5	6	7	9
NEW	16	6	1	2	3	7	8	9	4	10	5
OLD	17	2	3	4	8	10	1	5	6	7	9
NEW	17	6	1	2	3	7	8	9	4	10	5
OLD	18	2	3	4	8	10	1	5	6	7	9
NEW	18	6	1	2	3	7	8	9	4	10	5
OLD	19	2	3	4	8	10	1	5	6	7	9
NEW	19	6	1	2	3	7	8	9	4	10	5

Table 12. (Continued)

OLD	20	2	3	4	8	10	1	5	6	7	9
NEW	20	6	1	2	3	7	8	9	4	10	5
OLD	21	2	3	4	8	10	1	5	6	7	9
NEW	21	6	1	2	3	7	8	9	4	10	5
OLD	22	2	3	4	8	10	1	5	6	7	9
NEW	22	6	1	2	3	7	8	9	4	10	5
OLD	23	2	3	4	8	10	1	5	6	7	9
NEW	23	6	1	2	3	7	8	9	4	10	5
OLD	24	2	3	4	8	10	1	5	6	7	9
NEW	24	6	1	2	3	7	8	9	4	10	5
OLD	25	2	3	4	8	10	1	5	6	7	9
NEW	25	6	1	2	3	7	8	9	4	10	5
OLD	26	2	3	4	8	10	1	5	6	7	9
NEW	26	6	1	2	3	7	8	9	4	10	5
OLD	27	2	3	4	8	10	1	5	6	7	9
NEW	27	6	1	2	3	7	8	9	4	10	5
OLD	28	2	3	4	8	10	1	5	6	7	9
NEW	28	6	1	2	3	7	8	9	4	10	5
OLD	29	2	3	4	8	10	1	5	6	7	9
NEW	29	6	1	2	3	7	8	9	4	10	5
OLD	30	2	3	4	8	10	1	5	6	7	9
NEW	30	6	1	2	3	7	8	9	4	10	5
OLD	31	2	3	4	8	10	1	5	6	7	9
NEW	31	6	1	2	3	7	8	9	4	10	5

ROP-VP ARRAYS AND OTHER RELATED VARIABLES

I= 1	NPMAX= 10	NPMIN= 6	IMPW= 0	ICR= 0							
VP.DA (LNEW)	0.00000	0.00000	0.00000	0.00000	0.00000	.05199	.03642	.04545	.41995	.06387	0.00000
DRDOTP(LNEW)	0.00000	0.00000	0.00000	0.00000	0.00000	0.00000	.06818	.01774	.01774	.03549	
ROP (LOLD)	1.21783	1.29394	1.26802	1.28896	1.30881	1.29880	1.25330	1.19851	1.18342	1.15263	
VP (LOLD)	0.00000	0.00000	0.00000	0.00000	.40000	.50133	.60913	0.00000	.85593	0.00000	
I= 2	NPMAX= 10	NPMIN= 6	IMPW= 0	ICR= 0							
VP.DA (LNEW)	0.00000	0.00000	0.00000	0.00000	0.00000	.05199	.01644	.03321	.03864	.10874	0.00000
DRDOTP(LNEW)	0.00000	0.00000	0.00000	0.00000	0.00000	0.00000	.06818	.01774	.01774	.03549	
ROP (LOLD)	5.05043	.00001	.00001	.00001	4.14696	.53422	.45916	.00001	.35228	.00001	
VP (LOLD)	0.00000	0.00000	0.00000	0.00000	.36678	.48028	.60397	0.00000	.85909	0.00000	
I= 3	NPMAX= 10	NPMIN= 6	IMPW= 0	ICR= 0							
VP.DA (LNEW)	0.00000	0.00000	0.00000	0.00000	0.00000	.05199	.02257	.03819	.04901	.04698	0.00000
DRDOTP(LNEW)	0.00000	0.00000	0.00000	0.00000	0.00000	0.00000	.06818	.01774	.01774	.03549	
ROP (LOLD)	5.05165	.00001	.00001	.00001	3.02050	.46468	.36284	.00001	.75536	.00001	
VP (LOLD)	0.00000	0.00000	0.00000	0.00000	.33644	.44238	.62028	0.00000	.91669	0.00000	
I= 4	NPMAX= 10	NPMIN= 6	IMPW= 0	ICR= 0							
VP.DA (LNEW)	0.00000	0.00000	0.00000	0.00000	0.00000	.05199	.01733	.04384	.06608	.15738	0.00000
DRDOTP(LNEW)	0.00000	0.00000	0.00000	0.00000	0.00000	0.00000	.06818	.01774	.01774	.03549	
ROP (LOLD)	1.03363	.00001	.00001	.00001	3.03353	.46382	.26854	.00001	.22549	.00001	

Table 12. (Continued)

YP (LOLD)	0.00000	0.00000	0.00000	0.00000	.30516	.44639	.68135	0.00000	.94327	0.00000	
I= 5 NPMAX= 10	NPMIN= 6	IMPW= 0	ICR= 0								
VP.DA (LNEW)	0.00000	0.00000	0.00000	0.00000	0.00000	.05199	.01269	.04830	.12776	.10495	0.00000
DMDOTP(LNEW)	0.00000	0.00000	0.00000	0.00000	0.00000	0.00000	.06818	.01774	.01774	.03549	
ROP (LOLD)	5.60947	.00001	.00001	.00001	5.57306	.36741	.13689	.00001	.33815	.00001	
YP (LOLD)	0.00000	0.00000	0.00000	0.00000	.26882	.43255	.79041	0.00000	.95720	0.00000	
I= 6 NPMAX= 10	NPMIN= 6	IMPW= 0	ICR= 0								
VP.DA (LNEW)	0.00000	0.00000	0.00000	0.00000	0.00000	.05199	.00916	.05235	.22240	.08362	0.00000
DMDOTP(LNEW)	0.00000	0.00000	0.00000	0.00000	0.00000	0.00000	.06818	.01774	.01774	.03549	
ROP (LOLD)	5.53892	.00001	.00001	.00001	5.53892	.33896	.07978	.00001	.42442	.00001	
YP (LOLD)	0.00000	0.00000	0.00000	0.00000	.22674	.42490	.82840	0.00000	.98865	0.00000	
I= 7 NPMAX= 10	NPMIN= 6	IMPW= 1	ICR= 0								
VP.DA (LNEW)	0.00000	0.00000	0.00000	0.00000	0.00000	.05199	.00618	.05370	.24530	.10881	.00296
DMDOTP(LNEW)	0.00000	0.00000	0.00000	0.00000	0.00000	0.00000	.06818	.01774	.01774	.03495	
ROP (LOLD)	5.49457	.00001	.00001	.00001	5.49457	.33040	.07234	.00001	.31751	.00001	
YP (LOLD)	0.00000	0.00000	0.00000	0.00000	.17857	.43756	.85751	0.00000	1.00000	0.00000	
I= 8 NPMAX= 10	NPMIN= 6	IMPW= 1	ICR= 0								
VP.DA (LNEW)	0.00000	0.00000	0.00000	0.00000	0.00000	.05199	.00355	.17724	.06763	.07998	.01851
DMDOTP(LNEW)	0.00000	0.00000	0.00000	0.00000	0.00000	0.00000	.06818	.01774	.01774	.03052	
ROP (LOLD)	5.48304	.00001	.00001	.00001	5.48304	.10011	.26236	.00001	.38362	.00001	
YP (LOLD)	0.00000	0.00000	0.00000	0.00000	.12498	.75547	.88536	0.00000	1.00000	0.00000	
I= 9 NPMAX= 10	NPMIN= 6	IMPW= 1	ICR= 0								
VP.DA (LNEW)	0.00000	0.00000	0.00000	0.00000	0.00000	.05199	.00632	.36119	.06098	.05401	.00948
DMDOTP(LNEW)	0.00000	0.00000	0.00000	0.00000	0.00000	0.00000	.06818	.01774	.01774	.02596	
ROP (LOLD)	5.48106	.00001	.00001	.00001	5.48106	.04913	.29097	.00001	.48867	.00001	
YP (LOLD)	0.00000	0.00000	0.00000	0.00000	.07656	.81842	.91572	0.00000	1.00000	0.00000	
I= 10 NPMAX= 10	NPMIN= 6	IMPW= 1	ICR= 0								
VP.DA (LNEW)	0.00000	0.00000	0.00000	0.00000	0.00000	.05199	.00814	.41839	.06378	.03733	.00852
DMDOTP(LNEW)	0.00000	0.00000	0.00000	0.00000	0.00000	0.00000	.06818	.01774	.01774	.02114	
ROP (LOLD)	5.46384	.00001	.00001	.00001	5.46384	.04241	.27855	.00001	.56620	.00001	
YP (LOLD)	0.00000	0.00000	0.00000	0.00000	.05825	.85590	.94307	0.00000	1.00000	0.00000	
I= 11 NPMAX= 10	NPMIN= 6	IMPW= 1	ICR= 0								
VP.DA (LNEW)	0.00000	0.00000	0.00000	0.00000	0.00000	.05199	.01028	.44228	.06728	.02196	.00762
DMDOTP(LNEW)	0.00000	0.00000	0.00000	0.00000	0.00000	0.00000	.06818	.01774	.01774	.01569	
ROP (LOLD)	5.41797	.00001	.00001	.00001	5.41797	.04013	.26373	.00001	.71437	.00001	
YP (LOLD)	0.00000	0.00000	0.00000	0.00000	.05354	.88254	.96587	0.00000	1.00000	0.00000	
I= 12 NPMAX= 10	NPMIN= 6	IMPW= 1	ICR= 0								
VP.DA (LNEW)	0.00000	0.00000	0.00000	0.00000	0.00000	.05199	.01287	.44015	.07192	.00928	.00679
DMDOTP(LNEW)	0.00000	0.00000	0.00000	0.00000	0.00000	0.00000	.06818	.01774	.01774	.00906	
ROP (LOLD)	5.31588	.00001	.00001	.00001	5.29643	.04031	.24673	.00001	.97665	.00001	
YP (LOLD)	0.00000	0.00000	0.00000	0.00000	.05485	.90261	.98557	0.00000	1.00000	0.00000	
I= 13 NPMAX= 9	NPMIN= 6	IMPW= 1	ICR= 0								
VP.DA (LNEW)	0.00000	0.00000	0.00000	0.00000	0.00000	.05199	.01695	.42068	.07983	.00849	
DMDOTP(LNEW)	0.00000	0.00000	0.00000	0.00000	0.00000	0.00000	.06818	.01774	.01764	0.00000	
ROP (LOLD)	4.04114	.00001	.00001	.00001	4.02246	.04219	.22092	.00001	.00001	.00001	
YP (LOLD)	0.00000	0.00000	0.00000	0.00000	.06298	.91406	1.00000	0.00000	1.00000	0.00000	
I= 14 NPMAX= 9	NPMIN= 6	IMPW= 1	ICR= 0								
VP.DA (LNEW)	0.00000	0.00000	0.00000	0.00000	0.00000	.05199	.02829	.40371	.06517	.01288	
DMDOTP(LNEW)	0.00000	0.00000	0.00000	0.00000	0.00000	0.00000	.06818	.01774	.01473	0.00000	
ROP (LOLD)	2.43177	.00001	.00001	.00001	2.41054	.04395	.22597	.00001	.00001	.00001	

Table 12. (Continued)

YP (LOLD)	0.00000	0.00000	0.00000	0.00000	.08789	.93296	1.00000	0.00000	1.00000	0.00000
I= 15 NPMAX= 9	NPMIN= 6	IMPW= 1	ICR= 0							
VP.DA (LNEW)	0.00000	0.00000	0.00000	0.00000	0.00000	.05199	.03305	.35922	.05304	.01136
JMDOTP(LNEW)	0.00000	0.00000	0.00000	0.00000	0.00000	0.00000	.06818	.01774	.01213	0.00000
ROP (LOLD)	2.15334	.00001	.00001	.00001	2.06335	.09340	.22868	.00031	.00001	.00001
YP (LOLD)	0.00000	0.00000	0.00000	0.00000	.16991	.99027	1.00000	0.00000	1.00000	0.00000
I= 16 NPMAX= 9	NPMIN= 6	IMPW= 1	ICR= 0							
VP.DA (LNEW)	0.00000	0.00000	0.00000	0.00000	0.00000	.05199	.03613	.28128	.04237	.00999
JMDOTP(LNEW)	0.00000	0.00000	0.00000	0.00000	0.00000	0.00000	.06818	.01774	.00981	0.00000
ROP (LOLD)	2.15389	.00001	.00001	.00001	1.88734	.04338	.23163	.00031	.00001	.00001
YP (LOLD)	0.00000	0.00000	0.00000	0.00000	.34016	.95393	1.00000	0.00000	1.00000	0.00000
I= 17 NPMAX= 9	NPMIN= 6	IMPW= 1	ICR= 0							
VP.DA (LNEW)	0.00000	0.00000	0.00000	0.00000	0.00000	.05199	.03851	.22891	.03319	.00875
JMDOTP(LNEW)	0.00000	0.00000	0.00000	0.00000	0.00000	0.00000	.06818	.01774	.00776	0.00000
ROP (LOLD)	2.32276	.00001	.00001	.00001	1.77064	.07751	.23427	.00031	.00001	.00001
YP (LOLD)	0.00000	0.00000	0.00000	0.00000	.47728	.96248	1.00000	0.00000	1.00000	0.00000
I= 18 NPMAX= 9	NPMIN= 6	IMPW= 1	ICR= 0							
VP.DA (LNEW)	0.00000	0.00000	0.00000	0.00000	0.00000	.05199	.03231	.22231	.02234	.00765
JMDOTP(LNEW)	0.00000	0.00000	0.00000	0.00000	0.00000	0.00000	.06818	.01774	.00578	0.00000
ROP (LOLD)	2.87430	.00001	.00001	.00001	2.11027	.07982	.25887	.00031	.00001	.00001
YP (LOLD)	0.00000	0.00000	0.00000	0.00000	.50919	.97382	1.00000	0.00000	1.00000	0.00000
I= 19 NPMAX= 9	NPMIN= 6	IMPW= 1	ICR= 0							
VP.DA (LNEW)	0.00000	0.00000	0.00000	0.00000	0.00000	.05199	.03115	.22379	.01831	.01263
JMDOTP(LNEW)	0.00000	0.00000	0.00000	0.00000	0.00000	0.00000	.06818	.01774	.00268	0.00000
ROP (LOLD)	2.94754	.00001	.00001	.00001	2.18921	.07929	.25211	.00031	.00001	.00001
YP (LOLD)	0.00000	0.00000	0.00000	0.00000	.50748	.98697	1.00000	0.00000	1.00000	0.00000
I= 20 NPMAX= 9	NPMIN= 6	IMPW= 1	ICR= 0							
VP.DA (LNEW)	0.00000	0.00000	0.00000	0.00000	0.00000	.05199	.02908	.22022	.00271	.00876
JMDOTP(LNEW)	0.00000	0.00000	0.00000	0.00000	0.00000	0.00000	.06818	.01774	.00061	0.00000
ROP (LOLD)	3.08140	.00001	.00001	.00001	2.34502	.07775	.22663	.00031	.00001	.00001
YP (LOLD)	0.00000	0.00000	0.00000	0.00000	.49332	.99632	1.00000	0.00000	1.00000	0.00000
I= 21 NPMAX= 8	NPMIN= 6	IMPW= 1	ICR= 0							
VP.DA (LNEW)	0.00000	0.00000	0.00000	0.00000	0.00000	.05199	.02666	.22478	.00275	
JMDOTP(LNEW)	0.00000	0.00000	0.00000	0.00000	0.00000	0.00000	.06818	.01733	0.00000	0.00000
ROP (LOLD)	3.24961	.00001	.00001	.00001	2.55781	.07798	.19890	.00031	.00001	.00001
YP (LOLD)	0.00000	0.00000	0.00000	0.00000	.46571	1.00000	1.00000	0.00000	1.00000	0.00000
I= 22 NPMAX= 8	NPMIN= 6	IMPW= 1	ICR= 0							
VP.DA (LNEW)	0.00000	0.00000	0.00000	0.00000	0.00000	.05199	.02438	.21696	.00321	
JMDOTP(LNEW)	0.00000	0.00000	0.00000	0.00000	0.00000	0.00000	.06818	.01727	0.00000	0.00000
ROP (LOLD)	3.39228	.00001	.00001	.00001	2.79689	.07962	.19525	.00031	.00001	.00001
YP (LOLD)	0.00000	0.00000	0.00000	0.00000	.42395	1.00000	1.00000	0.00000	1.00000	0.00000
I= 23 NPMAX= 8	NPMIN= 6	IMPW= 1	ICR= 0							
VP.DA (LNEW)	0.00000	0.00000	0.00000	0.00000	0.00000	.05199	.02283	.21525	.00139	
JMDOTP(LNEW)	0.00000	0.00000	0.00000	0.00000	0.00000	0.00000	.06818	.01716	0.00000	0.00000
ROP (LOLD)	3.44996	.00001	.00001	.00001	2.98655	.07974	.18192	.00031	.00001	.00001
YP (LOLD)	0.00000	0.00000	0.00000	0.00000	.36939	1.00000	1.00000	0.00000	1.00000	0.00000
I= 24 NPMAX= 8	NPMIN= 6	IMPW= 0	ICR= 0							
VP.DA (LNEW)	0.00000	0.00000	0.00000	0.00000	0.00000	.05199	.02149	.22931	0.00000	
JMDOTP(LNEW)	0.00000	0.00000	0.00000	0.00000	0.00000	0.00000	.06818	.01716	0.00000	0.00000
ROP (LOLD)	3.53131	.00001	.00001	.00001	3.17249	.07943	.16501	.00001	.00001	.00001

Table 12. (Concluded)

```
YP     (LOLD)      0.00000   0.00000   0.00000   0.00000    .31054    .99400   1.00000   0.00000   1.00000   0.00000

I=  25     NPMAX=     8     NPMIN=    6     IMPW=     0     ICR=    0
VP.DA (LNEW)       0.00300   0.00300   0.00300   0.00300   0.00300    .05199    .02287    .24973   0.00000
JMDOTP(LNEW)       0.00300   0.00300   0.00300   0.00300   0.00300   0.00300    .06818    .01716   0.00000   0.00000
ROP    (LOLD)      3.22870    .00001    .00001    .00001   2.99094    .06473    .15512    .00001    .00001    .00001
YP     (LOLD)      0.00300   0.00300   0.00300   0.00300    .27651    .98730    .99396   0.00000    .99615   0.00000

I=  26     NPMAX=     8     NPMIN=    6     IMPW=     0     ICR=    0
VP.DA (LNEW)       0.00300   0.00300   0.00300   0.00300   0.00300    .05199    .02341    .26744   0.00000
JMDOTP(LNEW)       0.00300   0.00300   0.00300   0.00300   0.00300   0.00300    .06818    .01716   0.00000   0.00000
ROP    (LOLD)      3.13164    .00001    .00001    .00001   2.91234    .06418    .13103    .00001    .00001    .00001
YP     (LOLD)      0.00300   0.00300   0.00300   0.00300    .26145    .97784    .98861   0.00000    .99353   0.00000

I=  27     NPMAX=     8     NPMIN=    6     IMPW=     0     ICR=    0
VP.DA (LNEW)       0.00300   0.00300   0.00300   0.00300   0.00300    .05199    .02506    .28848   0.00000
JMDOTP(LNEW)       0.00300   0.00300   0.00300   0.00300   0.00300   0.00300    .06818    .01716   0.00000   0.00000
ROP    (LOLD)      2.70538    .00001    .00001    .00001   2.70538    .05450    .10759    .00001    .00001    .00001
YP     (LOLD)      0.00300   0.00300   0.00300   0.00300    .25136    .96592    .98120   0.00000    .98893   0.00000

I=  28     NPMAX=     8     NPMIN=    6     IMPW=     0     ICR=    0
VP.DA (LNEW)       0.00300   0.00300   0.00300   0.00300   0.00300    .05199    .02716    .31894   0.00000
JMDOTP(LNEW)       0.00300   0.00300   0.00300   0.00300   0.00300   0.00300    .06818    .01716   0.00000   0.00000
ROP    (LOLD)      2.02156    .00001    .00001    .00001   2.02156    .05520    .08767    .00001    .00001    .00001
YP     (LOLD)      0.00300   0.00300   0.00300   0.00300    .24563    .95144    .97180   0.00000    .98238   0.00000

I=  29     NPMAX=     8     NPMIN=    6     IMPW=     0     ICR=    0
VP.DA (LNEW)       0.00300   0.00300   0.00300   0.00300   0.00300    .05199    .02980    .33520   0.00000
JMDOTP(LNEW)       0.00300   0.00300   0.00300   0.00300   0.00300   0.00300    .06818    .01716   0.00000   0.00000
ROP    (LOLD)      1.43411    .00001    .00001    .00001   1.43411    .05120    .07090    .00001    .00001    .00001
YP     (LOLD)      0.00300   0.00300   0.00300   0.00300    .24232    .93504    .96084   0.00000    .97422   0.00000

I=  30     NPMAX=     8     NPMIN=    6     IMPW=     0     ICR=    0
VP.DA (LNEW)       0.00300   0.00300   0.00300   0.00300   0.00300    .05199    .03302    .36167   0.00000
JMDOTP(LNEW)       0.00300   0.00300   0.00300   0.00300   0.00300   0.00300    .06818    .01716   0.00000   0.00000
ROP    (LOLD)       .92926    .00001    .00001    .00001    .92926    .04746    .05753    .00001    .00001    .00001
YP     (LOLD)      0.00300   0.00300   0.00300   0.00300    .24157    .91779    .94888   0.00000    .96492   0.00000

I=  31     NPMAX=     8     NPMIN=    6     IMPW=     0     ICR=    0
VP.DA (LNEW)       0.00300   0.00300   0.00300   0.00300   0.00300    .05199    .03642    .38898   0.00000
JMDOTP(LNEW)       0.00300   0.00300   0.00300   0.00300   0.00300   0.00300    .06818    .01716   0.00000   0.00000
ROP    (LOLD)       .42441    .00001    .00001    .00001    .42441    .04412    .04688    .00001    .00001    .00001
YP     (LOLD)      0.00300   0.00300   0.00300   0.00300    .24274    .90048    .93653   0.00000    .95494   0.00000

     *** PARTICLE IMPACT -- K =  2  ***
```

calculations had not entirely converged by that time, still having small, residual transients. However, it has been found that the flowfield closely approaches steady-state in approximately 1,000 steps. Hence, a limit of 1,000 steps is usually sufficient for calculating particle impact conditions. The slow rate of final convergence is almost certainly caused by the low Mach numbers near the chamber boundaries. Substantial improvements in the rate of convergence would require the development of new calculation procedures in the low Mach number regime.

Figure 5 shows the CFC mesh geometry for the sample problem, and Figure 6 shows the trajectories for the three particle size groups evaluated.

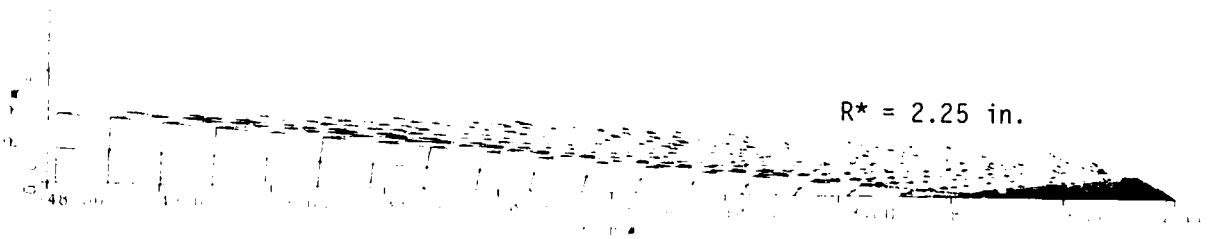

Figure 5. CFC Mesh Geometry for the NTF 001 at 0 Sec Burn Time

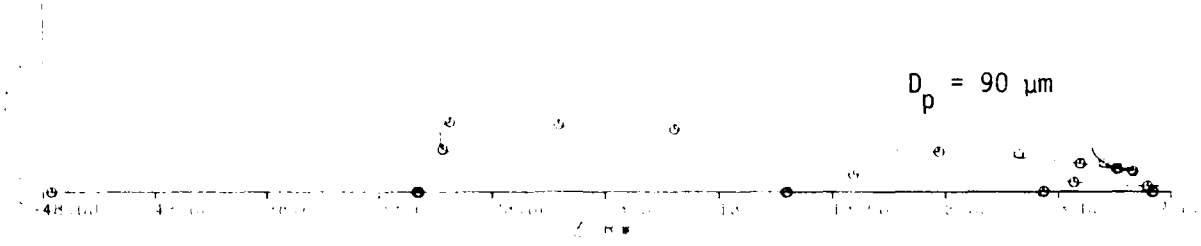

(a) Particle Size Group 1

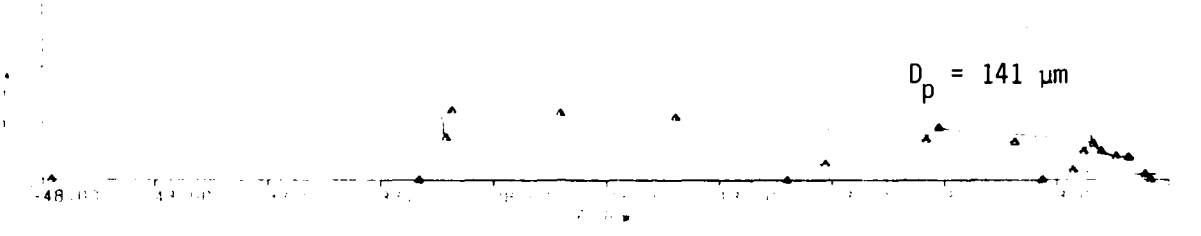

(b) Particle Size Group 2

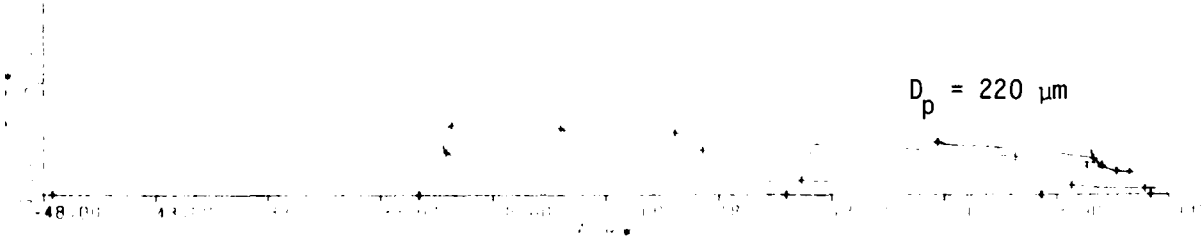

(c) Particle Size Group 3

Figure 6. Particle Trajectories for the NTF 001 Demonstration at 0 Sec Burn Time

P. 86 BLANK

PART 2

CHARRING MATERIAL ABLATION-EROSION (CMAE) CODE

SECTION 8

CMAE ANALYTICAL BASIS

Particle erosion is coupled with gas-surface thermochemical ablation in the nozzle entrance and throat regions. A comprehensive procedure already existed to predict recession in rocket nozzles due to ablation alone (References 12 and 13). The procedure was modified to account for the effects of impact erosion. It was assumed that particulate erosion did not affect the thermochemistry, kinetics, and boundary layer aspects of the calculation procedure. Hence, the only modifications required were to the recession calculations. The CFC provides the impact parameters which are input to the CMAE code.

The base code for the recession calculations was the Charring Material Ablation (CMA) code (Reference 5). The new code calculates mass loss due to both erosion and ablation; hence, it was called the Charring Material Ablation-Erosion (CMAE) code. The major modifications to the code were inclusion of a subroutine to calculate the erosion contribution, and modification to the surface energy balance to include erosion effects. The erosion contribution is calculated using the model for mechanical and chemical erosion described in Reference 1. The modification to the surface energy balance is discussed below. Again, it is assumed that the reader is familiar with the basic concepts and procedure (References 12 and 13).

PREVIOUS PAGE IS BLANK

Erosion Model

The erosion model in CMAE is in the form of a G-law with two components: mechanical erosion due to mechanical mass removal, and chemical erosion due to chemical reactions between molten particles and the surface. G, which is the ratio of mass flux of material removed to mass flux of incident particles, can be related to particle impact conditions (Reference 11), as follows:

$$G = a\, V_p^b\, D_p^c\, (\sin \alpha)^d\, T^e \qquad (22)$$

where

V_p = particle impact velocity

D_p = diameter of impacting particles

α = angle of impact relative to the surface

T = target temperature

a, b, c, d, e are empirically determined constants

Each of the mechanical and chemical components of erosion, G_{mech} and G_{chem} are in the form of Equation (22); the total erosion being given by the sum of the two components. A special form of the temperature dependence was formulated for rocket nozzle erosion. The limited data available on temperature indicated that no erosion occurred below 3,000°R (T_1) and that erosion was essentially independent of temperature above 4,500°R (T_2). The functional dependence of erosion on temperature between these two limits was assumed to be smooth and was modeled by the hyperbolic tangent function:

$$f(T) = \frac{1}{2}\left[\tanh\left(\frac{T - T_o}{\Delta T}\right) + 1\right] \tag{23}$$

where

$T_o = \frac{T_1 + T_2}{2}$, the midpoint between the temperature limits

$\Delta T = n(T_2 - T_1)$, a stretching parameter. (The recommended value of n is 1/4.)

The G-law used in the CMAE code incorporates both the power law and the hyperbolic tangent forms of temperature dependence, as follows:

$$G = a\, V_p^b\, D_p^c\, (\sin\alpha)^d\, T^e\, f(T) \tag{24}$$

The user, therefore, has the option of selecting the hyperbolic-tangent function (by setting e = 0), or the power-law function (by setting $T_o = 0$), or any combination of the two.

Since the combined effect of erosion and ablation is important, the CMA surface energy balance was modified to account for the coupling between the two mechanisms. As shown in the following section, he surface energy balance is modified only by one term: $\Sigma\, \dot{m}_{e_{chem}} \Delta H_R$, where $\dot{m}_{e_{chem}}$ is the mass flux removed due to chemical erosion, ΔH_R is the heat of reaction and Σ signifies summation over all particle types and sizes. The value of $\dot{m}_{e_{chem}}$ is calculated from the G-law for chemical erosion, and ΔH_R is an input variable.

The addition of this new term affects the other energy balance parameters. In particular, the conduction term is directly affected since it is influenced by the recession rate. It is, therefore, important to account

for the couple effects of ablation, erosion, and in-depth conduction in calculating the total recession in the entrance and throat regions of rocket nozzles.

Surface Energy Balance

The surface energy balance (SEB) was modified in the new (CMAE) code to include the energy fluxes associated with particle erosion effects. The formulation is similar to the one used in the ABRES Shape Change Code (ASCC) (Reference 11). The following sketch illustrates an ablating-eroding surface, receding with the rate $\dot{s}$ in the surface normal direction. A differential control volume is fixed to the surface. The important energy fluxes, including erosion-related terms, to and from the surface are shown.

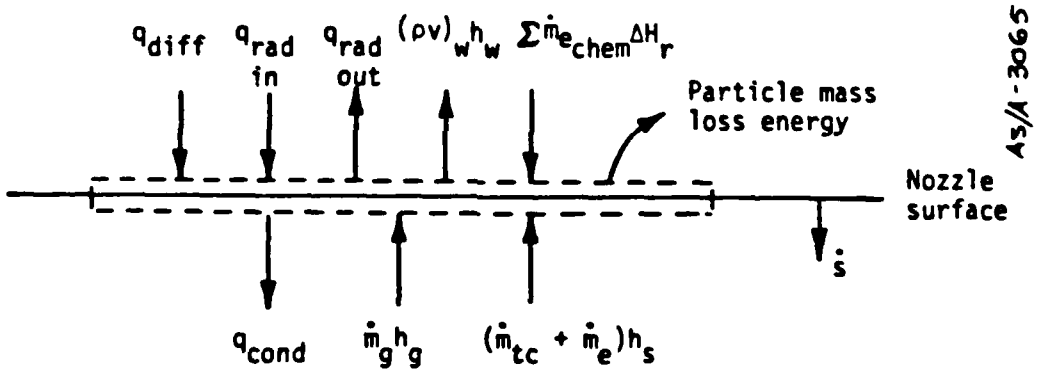

The energy inputs to the control volume include the following:

- The diffusive energy fluxes from the boundary layer, q_{diff}
- The radiative energy absorbed by the surface, $q_{rad_{in}}$
- The energy released due to chemical interactions of the particles with the surface, $\Sigma \dot{m}_{e_{chem}} \Delta H_r$, where ΔH_r is the heat of reaction $\dot{m}_{e_{chem}}$ is the mass flux removed due to chemical erosion, and the Σ signifies summation over all particle types and sizes

- The enthalpy flux carried to the surface by the pyrolysis gases, $\dot{m}_g h_g$, where $\dot{m}_g$ and h_g are the mass flux and enthalpy, respectively, of the pyrolysis gases
- The energy flux due to the relative motion of the control volume, $(\dot{m}_{tc} + \dot{m}_e) h_s$, where $\dot{m}_{tc}$ is the mass flux of the surface removed due to thermochemical ablation, $\dot{m}_e$ is the mass removed due to erosion, and h_s is the sensible enthalpy of the solid material at the surface

The energy fluxes leaving the control volume include the following:

- The energy flux carried into the material due to conduction, q_{cond}
- The radiative energy flux emitted by the surface, $q_{\substack{rad \\ out}}$
- The energy carried away due to gross blowing at the surface, $(\rho v)_w h_w$, where $(\rho v)_w$ is the blowing mass flux, $(\rho v)_w = \dot{m}_{tc} + \dot{m}_g$, and h_w is the enthalpy of the blown gases at the surface
- The energy flux lost from the surface due to erosive mass removal

The last item equals the product of the mass flux removed due to erosion, $\dot{m}_e$, and the sensible enthalpy of the surface material, h_s. Hence, the surface energy balance can be written as:

$$q_{diff} + q_{\substack{rad \\ in}} + \sum \dot{m}_{e_{chem}} \Delta H_r + \dot{m}_g h_g + \dot{m}_{tc} h_s + \dot{m}_e h_s$$

$$= q_{cond} + q_{\substack{rad \\ out}} + (\dot{m}_{tc} + \dot{m}_g) h_w + \dot{m}_e h_s \qquad (25)$$

The final terms on each side of the equation cancel out, leaving the chemical interactions term as the only new term in the modified surface energy balance.

However, erosion influences most of the remaining terms in the SEB. Conduction is directly affected, since conduction in a moving medium depends upon the rate of movement of the medium. The other terms are indirectly affected since they must be adjusted in order to maintain an energy balance at the surface.

The modified SEB solves for the wall temperature and the recession rate. An interative procedure is used to solve implicitly for the unknowns at each time step. The procedure is identical to the one used in the base (CMA) code except that the erosion calculation routine is included in the implicit procedure.

SECTION 9

CMAE INPUT

This section describes only the new input required for CMAE, which is inserted between the CMA surface time-dependent boundary conditions and the surface thermochemistry tables. The erosion input contains a control card describing the number of impacting particle groups, the number of particle types, and the names of those particle types. If no erosion is desired, a blank card must be input to denote zero particles. After the control card, the following data are input: a set of particle time histories for each particle; the coefficients for the mechanical erosion-mass loss law; and the coefficients for the chemical erosion-mass loss law and the temperature dependent heats of reaction for each particle type. The formats for each of the card set types are described below:

Control Card

Column	Format	Variable Description	Units
1-5	I5	Number of particle groups (max = 10)	None
6-10	I5	Number of particle types (max = 2)	None
11-15	A5	Alphanumeric description of particle type 1	None
16-20	A5	Alphanumeric description of particle type 2	None

Particle Group Time History

One card set for each particle group is required.

Card Number	Column	Format	Variable Description	Units
1	1-5	I5	Particle type (1 or 2)	None
	11-20	F10.0	Diameter of particle	μm
2+	1	I1	Flag, nominally blank, punched to indicate last card of time table	None
	2-10	F9.0	Time	sec
	11-20	F10.0	Impacting mass flux	lbm/ft^2-sec
	21-30	F10.0	Particle impact velocity	ft/sec
	31-40	F10.0	Particle impact angle	deg

Mechanical Erosion-Mass Removal Law

These coefficients correspond to those in Equations (22) and (23) for mechanical erosion.

Column	Format	Variable Description	Units
1-10	F10.0	a	None
11-20	F10.0	b	None
21-30	F10.0	c	None
31-40	F10.0	d	None
41-50	F10.0	e	None
51-60	F10.0	T_o	°R
61-70	F10.0	ΔT	°R

Chemical Erosion-Mass Removal Law and Energy

One card set for each particle type is required. The coefficients correspond to those in Equation (23) for chemical erosion. (The same temperatures, T_o and ΔT, are used from above.)

Card Number	Column	Format	Variable Description	Units
1	1-10	F10.0	a	None
	11-20	F10.0	b	None
	21-30	F10.0	c	None
	31-40	F10.0	d	None
	41-50	F10.0	e	None
2+	1	I1	Flag, nominally blank, punched to indicate last card of temperature table	None
	2-10	F9.0	Temperature	°R
	11-21	F10.0	Heat of reaction for the following reaction: $n\ \text{Particle} + C^* \longrightarrow \text{Product} + \Delta H_R$	Btu/lb-carbon

P. 98 BLANK

SECTION 10

SAMPLE PROBLEM USING CMAE

The calculation for total recession in the nozzle entrance region of the NTF 001 firing is presented here as a sample problem. The firing results were used to demonstrate the subsonic-transonic total recession prediction methodology developed for the Particle Impact Erosion program, as described in Reference 1.

Table 13 presents the CMAE input, while Table 14 illustrates the new output of erosion data and recession-temperature at selected times.

PREVIOUS PAGE IS BLANK

Table 13. CMAE Sample Problem Input

```
CMA ANALYSIS OF PITCH FIBER NTF001 NOZZLE WITH PARTICLE EROSION
FORWARD LOCATION THROAT  2.25 IN RADIUS  1.68 IN THICK
THERMOCHEMISTRY BASED ON HTPB -- WITH AL2O3  2 MIL ROUGH  NTF001ER
A                1.          0.          1.          1.          1.        90000.
B             1.             0.          1.          1.          1.        90000.
C          220.74          120.74         1.          1.          1.         90000.
10 24        0.0            63.4          .1          1.0         2.5                    .4
   1.0      25.0            .004          0.          0.          0.          0.        536.
 2     530.                 .002       2.91578
 2     530.                 .004
 2     530.                 .006
 2     530.                 .008
 2     530.                 .010
 2     530.                 .012
 2     530.                 .014
 2     530.                 .016
 2     530.                 .018
 2     530.                 .020
 2     530.                 .030
 2     530.                 .040
 2     530.                 .050
 2     530.                 .060
 2     530.                 .170
 2     530.                 .20
 2     530.                 .25
 2     530.                 .25
 2     530.                 .25
 2     530.                 .25
 3     530.                 .25
 3     530.                 .25
 3     530.                 .25
 3     530.                 .25

    530.        .15         .01339      .7115
    960.        .31         .01105      .7115
   1460.        .39         .008969     .7115
   1960.        .43         .007697     .7115
   2460.        .465        .006342     .7115
   2960.        .485        .005556     .7115
   3460.        .505        .005161     .7115
   3960.        .515        .005069     .7115
   4460.        .520        .005047     .7115
   4960.        .526        .005047     .7115
-1 7460.        .526        .005047     .7115
    530.        .15         .01339      .7115
    960.        .31         .01105      .7115
   1460.        .39         .008969     .7115
   1960.        .43         .007697     .7115
   2460.        .465        .006342     .7115
   2960.        .485        .005556     .7115
   3460.        .505        .005161     .7115
   3960.        .515        .005069     .7115
   4460.        .520        .005047     .7115
   4960.        .526        .005047     .7115
-1 7460.        .526        .005047     .7115
```

Table 13. (Continued)

```
 108.2
  500.        .210        .760-4
 1000.        .362        .750-4
 1500.        .555        .380-4
 2000.        .735        .650-4
 3000.        .687        .160-4
 4000.        .630        .340-3
 5000.        .590        .735-3
 6000.        .590        .136-2
19999.        .590        .136-2
1   0.0    7000.
      0.0      0.0
      0.0  -1436.27      416.54  1.56425  55.569
   10.0    -1436.27      416.54  1.56425  55.569
1  63.4    -1436.27      416.54  1.56425  55.569
     3    1  At
     1       90.12
    0.0       9.91     615.87     22.174
   20.0       0.00     615.87     22.174
   40.0       0.00     615.87     22.174
1  65.0       0.00     615.87     22.174
     1      191.25
    0.0      12.01     568.54     23.6805
   20.0       3.67     541.12     12.582
   40.0       0.00     541.12     12.582
1  65.0       0.00     541.12     12.582
     1      204.85
    0.0      12.96     521.41     25.653
   20.0      14.87     527.07     12.825
   40.0       0.00     527.07     12.825
1  65.0       0.00     527.07     12.825
   .641E-5    .7987      1.236      .2992      0.     3750.      375.
  .1335E-3    .8          .8         .8        0.
   900.    -24700.
  1650.    -24500.
  1655.    -24200.
  4970.    -23000.
  4975.    -12500.
1 7200.    -12250.
  .68439      1.0                                                    1
 55.5690 0.0      0.0     500.00000.667 -825.176-1899.741-1  CHAR      0.5010+00
 55.5690 0.0      0.0    1000.00000.667 -561.750-1726.032-1  CHAR      0.5010+00
 55.5690 0.0      0.0    1500.00000.667 -278.856-1537.637-1  CHAR      0.5010+00
 55.5690 0.0      0.0    2000.00000.667   20.489-1338.908-1  CHAR      0.5010+00
 55.5690 0.0      0.0    2500.00000.667  335.680-1037.704-1  CHAR      0.5010+00
 55.5690 0.0      0.0    3000.00000.667  662.435 -822.667-1  CHAR      0.5010+00
 55.5690 0.0      0.0    3500.00000.667  995.749 -604.988-1  CHAR      0.5010+00
 55.5690 0.0      0.0    4000.00000.667 1334.797 -385.024-1  CHAR      0.5010 00
 55.569  1.07056 0.00001 298.      .667-1000.    -1000.      1  CHAR
 55.5690 1.07056 0.00002 500.00000.667-1559.878-1467.181  1  CHAR      0.0
 55.5690 1.07056 0.000031000.00000.667-1075.703-1114.499  1  CHAR      0.0
 55.5690 1.07056 0.000421200.00000.667 -693.430 -819.564  1  C*        0.0
 55.5690 1.07056 0.001261400.00000.667 -472.767 -645.031  1  C*        0.0
 55.5690 1.07056 0.002481600.00000.667 -340.633 -540.906  1  C*        0.0
 55.5690 1.07056 0.004091800.00000.667 -212.769 -442.036  1  C*        0.0
```

Table 13. (Concluded)

```
55.5690 1.07056 0.006082000.00000.667  -81.127 -341.562 1  C*        0.0
55.5690 1.07056 0.008532200.00000.667   56.393 -237.973 1  C*        0.0
55.5690 1.07056 0.012102400.00000.667  204.462 -128.730 1  C*        0.0
55.5690 1.07056 0.019682600.00000.667  377.227   -4.823 1  C*        0.0
55.5690 1.07056 0.040792800.00000.667  612.288  158.910 1  C*        0.0
55.5690 1.07056 0.103943000.00000.667 1003.606  426.447 1  C*        0.0
55.5690 1.07056 0.160303200.00000.667 1372.009  738.733 1  C*        0.0
55.5690 1.07056 0.233213400.00000.667 1807.347 1123.301 1  C*        0.0
55.5690 1.07056 0.363623600.00000.667 2383.177 1671.913 1  C*        0.0
55.5690 1.07056 0.605613800.00000.667 3095.004 2401.100 1  C*        0.0
55.5690 1.07056 1.013804000.00000.667 3828.351 3192.795 1  C*        0.0
55.569  0.00000 0.00001 298.      .667-1800.   -1800.     1  CHAR
55.5690 0.00000 0.00002 500.00000.667-1559.678-1467.181 1  CHAR      0.0
55.5690 0.00000 0.000031000.00000.667-1075.703-1114.499 1  CHAR      0.0
55.5690 0.00000 0.000421200.00000.667 -693.430 -819.564 1  C*        0.0
55.5690 0.00000 0.001261400.00000.667 -472.767 -645.091 1  C*        0.0
55.5690 0.00000 0.002481600.00000.667 -340.633 -540.906 1  C*        0.0
55.5690 0.00000 0.004091800.00000.667 -212.769 -442.036 1  C*        0.0
55.5690 0.00000 0.006082000.00000.667  -81.127 -341.562 1  C*        0.0
55.5690 0.00000 0.008532200.00000.667   56.393 -237.973 1  C*        0.0
55.5690 0.00000 0.012102400.00000.667  204.462 -128.730 1  C*        0.0
55.5690 0.00000 0.019682600.00000.667  377.227   -4.823 1  C*        0.0
55.5690 0.00000 0.040792800.00000.667  612.288  158.910 1  C*        0.0
55.5690 0.00000 0.103943000.00000.667 1003.606  426.447 1  C*        0.0
55.5690 0.00000 0.160303200.00000.667 1372.009  738.733 1  C*        0.0
55.5690 0.00000 0.233213400.00000.667 1807.347 1123.301 1  C*        0.0
55.5690 0.00000 0.363623600.00000.667 2383.177 1671.913 1  C*        0.0
55.5690 0.00000 0.605613800.00000.667 3095.004 2401.100 1  C*        0.0
```

Table 14. CMAE Sample Problem Output

---EROSION MODEL INPUT---

PARTICLE NO. 1 PARTICLE TYPE AL PARTICLE DIAM. = 90.1 MICRONS

TIME	MASS FLUX (LBM/FT2-SEC)	VELOCITY (FT/SEC)	ANGLE (DEG)
0.0	9.91000	615.870000	22.174
20.000	.0	615.870000	22.174
40.000	.0	615.870000	22.174
65.000	.0	615.870000	22.174

PARTICLE NO. 2 PARTICLE TYPE AL PARTICLE DIAM. = 131.2 MICRONS

TIME	MASS FLUX (LBM/FT2-SEC)	VELOCITY (FT/SEC)	ANGLE (DEG)
0.0	12.0100	560.540000	23.600
20.000	3.67000	541.120000	12.582
40.000	.0	541.120000	12.582
65.000	.0	541.120000	12.582

PARTICLE NO. 3 PARTICLE TYPE AL PARTICLE DIAM. = 204.8 MICRONS

TIME	MASS FLUX (LBM/FT2-SEC)	VELOCITY (FT/SEC)	ANGLE (DEG)
0.0	12.9600	521.410000	25.653
20.000	14.8700	527.070000	12.825
40.000	.0	527.070000	12.825
65.000	.0	527.070000	12.825

Table 14. (Continued)

---G-LAW CONSTANTS---

G = A * DPART ** B * VELOCITY ** C * SIN(ANGLE) ** D * TEMP ** E

MODEL	A	B	C	D	E	TYPE
EROSION						
	.8410000-05	.798700	1.23600	.299200	.0	
CHEMICAL						
	.1335000-03	.800000	.800000	.800000	.0	AL

G-LAW LINEAR TEMPERATURE RAMP (DEGR)

TMPSTR = 3750.00 TMPSTP = 375.00

CHEMICAL ENERGY TABLES

PART	TEMP (DEGR)	ENERGY (BTU/LBM CARB)
AL		
	900.00	-24700.0
	1650.00	-24500.0
	1655.00	-24200.0
	4970.00	-23000.0
	4975.00	-12500.0
	7200.00	-12250.0

---SURFACE EQUILIBRIUM DATA---

RATIO OF MASS TO HEAT TRANSFER COEFFICIENTS = 0.684
UNEQUAL DIFFUSION EXPONENT = 0.667
NOMINAL SURFACE VIEW FACTOR = 1.000 (OPTION 1)
FISSURE MODEL NOT USED FOR GAS TERMS
NO RADIUS CORRECTION ON CM
NO CHAR SWELL CORRECTION ON SURFACE RECESSION

Table 14. (Continued)

20.0000 SECONDS

TIME STEP	SURF ITER	PROB OPTN	SURFACE RAD (IN)	M WALL (BTU/LB)	M EDGE (BTU/LB)	HEAT COEFF (LB/SQ FT-SEC)	CM/CMO
1723	3	1	3.3195	-2685.05	-1436.27	1.5631	0.99929

---ABLATION RATES---

B PRIME	B PRIME G	M DOT CHAR (LB/SQ FT-SEC)	M DOT GAS (LB/SQ FT-SEC)	M CHAR (LB/ORIG SQ FT)	M GAS (LB/ORIG SQ FT)
0.00267	0.0	0.002855	0.0	4.343427	0.0

---RECESSIONS/RECESSION RATES---

SURFACE (IN) / (IN/SEC)	CHAR (0.02)	PYROLYSIS (0.98)
0.4037097/0.0219391	1.6797929/-.0011564	1.6797929/-.0011564

---SURFACE ENERGY FLUX TERMS---

CURRENT RATES (BTU/SQ FT SURFACE-SEC)
AND INTEGRATED VALUES (BTU/ORIG SQ FT)

	CONVECTED IN	RADIATED IN	RADIATED OUT	CHEMICAL GENERATION	CONDUCTION AWAY
RATE	0.1950D+04	0.296D+03	0.253D+02	0.234D+03	0.438D+03
TOTAL	0.430D+05	0.631D+04	0.459D+03	0.521D+04	0.983D+04

---INTERIOR ENERGY TERMS---

CURRENT RATES (BTU/SQ FT SURFACE-SEC)
AND INTEGRATED VALUES (BTU/ORIG SQ FT)

	PYROL GAS PICK UP	DECOMP ABSORPTION	CONVECTION WITH SOLIDS	STORAGE IN SOLID	LOSS AT REAR FACE
RATE	0.0	0.0	0.187D+03	0.242D+03	0.646D+01
TOTAL	0.0	0.0	0.368D+04	0.607D+04	0.708D+02

NODE	MAT	TEMP (DEG R)	DENSITY (LB/CU FT)	ENTHALPY (BTU/LB)	NODE	MAT	TEMP (DEG R)	DENSITY (LB/CU FT)	ENTHALPY (BTU/LB)
1	2	2932.67	120.740	925.79	13	2	2177.72	120.740	574.95
2	2	2908.97	120.740	914.25	14	2	2025.10	120.740	506.69
3	2	2880.60	120.740	901.06	15	2	1797.11	120.740	410.73
4	2	2844.89	120.740	884.09	16	2	1558.13	120.740	312.75
5	2	2801.95	120.740	863.70	17	2	1372.79	120.740	242.00
6	2	2752.17	120.740	840.05	18	2	1262.53	120.740	203.41
7	2	2696.02	120.740	813.38	19	2	1236.15	120.740	194.17
8	2	2634.23	120.740	784.03	21	3	610.29	108.200	0.0
9	2	2567.68	120.740	752.42	22	3	533.46	108.200	0.0
10	2	2497.30	120.740	718.99	23	3	530.11	108.200	0.0
11	2	2411.18	120.740	679.42	24	3	530.00	108.200	0.0
12	2	2301.92	120.740	630.53					

Table 14. (Continued)

20.0000 SECONDS

TIME STEP	SURF ITER	PROB OPTN	SURFACE RAD (IN)	H WALL (BTU/LB)	H EDGE (BTU/LB)	HEAT COEFF (LB/SQ FT-SEC)	CH/CHO
1723	3	1	3.3195	-2685.05	-1436.27	1.5631	0.99929

---CHEMICAL EROSION ENERGY---
RATE (BTU/SQ FT-SEC)

-0.2018D+04

---MASS LOSS SUMMARY---

	MASS FLUX (LB/SQ FT-SEC)	RECESSION RATE (IN/SEC)	RECESSION (IN)
THERMOCHEMICAL ABLATION	0.2855D-02	0.2837D-03	0.4669D-02
PARTICLE MECHANICAL EROSION	0.1328D+00	0.1320D-01	0.2171D+00
PARTICLE CHEMICAL EROSION	0.6501D-01	0.6449D-02	0.1720D+00
TOTAL	0.2207D+00	0.2194D-01	0.4037D+00

Table 14. (Continued)

63.4000 SECONDS

TIME STEP	SURF ITER	PROB OPTN	SURFACE RAD (IN)	M WALL (BTU/LB)	M EDGE (BTU/LB)	HEAT COEFF (LB/SQ FT-SEC)	CH/CHO
3716	3	1	3.8475	-1608.58	-1436.27	1.5453	0.98789

---ABLATION RATES---

B PRIME	B PRIME G	M DOT CHAR (LB/SQ FT-SEC)	M DOT GAS	M CHAR (LB/ORIG SQ FT)	M GAS
0.04499	0.0	0.047583	0.0	10.873561	0.0

---RECESSIONS/RECESSION RATES---
(IN) / (IN/SEC)

SURFACE	CHAR (0.02)	PYROLYSIS (0.98)
0.9317619/0.0047291	1.6796082/-.0000018	1.6796082/-.0000018

---SURFACE ENERGY FLUX TERMS---
CURRENT RATES (BTU/SQ FT SURFACE-SEC)
AND INTEGRATED VALUES (BTU/ORIG SQ FT)

	CONVECTED IN	RADIATED IN	RADIATED OUT	CHEMICAL GENERATION	CONDUCTION AWAY
RATE	0.266D+03	0.296D+03	0.228D+03	-0.124D+03	0.211D+03
TOTAL	0.979D+05	0.226D+05	0.769D+04	0.890D+04	0.287D+05

---INTERIOR ENERGY TERMS---
CURRENT RATES (BTU/SQ FT SURFACE-SEC)
AND INTEGRATED VALUES (BTU/ORIG SQ FT)

	PYROL GAS PICK UP	DECOMP ABSORPTION	CONVECTION WITH SOLIDS	STORAGE IN SOLID	LOSS AT REAR FACE
RATE	0.0	0.0	0.379D+02	0.154D+03	0.188D+02
TOTAL	0.0	0.0	0.879D+04	0.191D+05	0.779D+03

NODE	MAT	TEMP (DEG R)	DENSITY (LB/CU FT)	ENTHALPY (BTU/LB)	NODE	MAT	TEMP (DEG R)	DENSITY (LB/CU FT)	ENTHALPY (BTU/LB)
1	2	5077.73	120.740	2023.45	12	2	4561.76	120.740	1753.24
2	2	5069.84	120.740	2016.14	13	2	4433.20	120.740	1686.15
3	2	5046.55	120.740	2007.05	14	2	4261.80	120.740	1597.45
4	2	5022.47	120.740	1994.38	15	2	3981.12	120.740	1452.20
5	2	4991.71	120.740	1978.20	16	2	3705.56	120.740	1311.51
6	2	4954.45	120.740	1958.62	17	2	3627.18	120.740	1271.53
7	2	4910.88	120.740	1935.83	21	3	1143.76	108.200	0.0
8	2	4861.27	120.740	1909.88	22	3	606.90	108.200	0.0
9	2	4805.90	120.740	1880.93	23	3	538.28	108.200	0.0
10	2	4745.15	120.740	1849.15	24	3	530.78	108.200	0.0
11	2	4867.12	120.740	1808.34					

Table 14. (Concluded)

63.4000 SECONDS

TIME STEP	SURF ITER	PROB OPTN	SURFACE RAD (IN)	H WALL (BTU/LB)	H EDGE (BTU/LB)	HEAT COEFF (LB/SQ FT-SEC)	CH/CHC
3716	3	1	3.8475	-1608.58	-1436.27	1.5453	0.98789

---CHEMICAL EROSION ENERGY---

RATE (BTU/SQ FT-SEC)
0.0

---MASS LOSS SUMMARY---

	MASS FLUX (LB/SQ FT-SEC)	RECESSION RATE (IN/SEC)	RECESSION (IN)
THERMOCHEMICAL ABLATION	0.4758D-01	0.4729D-02	0.1030D+00
PARTICLE MECHANICAL EROSION	0.0	0.0	0.4891D+00
PARTICLE CHEMICAL EROSION	0.0	0.0	0.3397D+00
TOTAL	0.4758D-01	0.4729D-02	0.9316D+00

SECTION 11

REFERENCES

1. Chiba, Z., P. A. Johnson, and M. J. Abbett, "Particle Impact Erosion, Volume 1, Recession Prediction Methodology for Rocket Nozzle Entrance and Throat Regions," AFRPL-TR-83-0013, May 1983.

2. Mockenhaupt, J. D., and J. H. Wickman, "Particle Impact Erosion, Volume II: Erosion Model Development (Expansion Region)," AFRPL-TR-83-0013, May 1983.

3. Mockenhaupt, J. D., and J. H. Wickman, "Particle Impact Erossion, Volume IV: User's Manual -- Erosion Prediction Procedure for Rocket Nozzle Expansion Region, AFRPL-TR-83-0013, May 1983.

4. Nickersen, G. R., D. F. Coates, and R. W. Hermsen, "A Computer Program for the Prediction of Solid Propellant Rocket Motor Performance," Interim Technical Report, AFRPL-TR-80-34, April 1981.

5. "User's Manual: Aerotherm Charring Material Thermal Response and Ablation Program, Version 3," Aerotherm Report No. UM-70-14, AFRPL-TR-70-92, April 1970.

6. Coons, S. A., "Surfaces for Computer-Aided Design of Space Forms," Project MAC, M.I.T., Report No. MAC-TR-41, June 1967 (First Published in 1964).

7. Cook, W. A., "Body Oriented (Natural) Coordinates for Generating Three-Dimensional Meshes," Int. J. Numerical Methods in Eng., Volume 8, 1974.

8. Zucrow, M. J. and J. D. Hoffman, Gas Dynamics, Volume II, John Wiley and Sons, New York, 1977.

9. "User's Manual: Aerotherm Chemical Equilibrium (ACE) Computer Program," Aerotherm Report No. UM-75-68, December 1975.

10. Kutler, P. and L. Sakell, "Three-Dimensional, Shock-on-Shock Interaction Problem," AIAA Journal, Vol. 13, No. 10, pp. 1,360-1,367, October 1975.

11. Rafinejad, D., et al., "Passive Nosetip Technology (PANT II) Program, Volume II --Computer User's Manual: ABRES Shape Change Code (ASCC)," Aerotherm/Acurex Corporation Report, SAMSO-TR-77-11, October 1976.

12. Tong, H., G. Hartman, E. Chu, and A. Murphy, "AFRPL Graphite Performance Prediction Program," Final Report, Aerotherm Report No. TR-76-16, AFRPL-TR-76-70, December 1976.

13. Johnson, P., H. Tong, G. Wallace, K. Kwong, E. Chu, and E. Fretter, "Graphite Performance Prediction Program," Acurex Final Report No. 78-291, AFRPL-TR-78-78, December 1978.